https://dx.doi.org/10.1016/j.apnum.2023.05.004

Stability and convergence analysis of the exponential time differencing scheme for a Cahn–Hilliard binary fluid-surfactant model

Yuzhuo Dong[a], Xiao Li[b], Zhonghua Qiao[b], Zhengru Zhang[a,c]

[a] *School of Mathematical Sciences, Beijing Normal University, Beijing 100875, China*
[b] *Department of Applied Mathematics, The Hong Kong Polytechnic University, Hung Hom, Kowloon, Hong Kong*
[c] *Laboratory of Mathematics and Complex Systems, Ministry of Education, Beijing 100875, China*

Abstract

In this paper, we focus on the Cahn–Hilliard type of binary fluid-surfactant model, which is derived as the H^{-1} gradient flow system of a binary energy functional of the fluid density and the surfactant density. By introducing two stabilization terms appropriately, we give a linear convex splitting of the energy functional, and then establish the exponential time differencing scheme with first-order temporal accuracy in combination with the Fourier spectral approximation in space. To guarantee the energy stability, we treat the nonlinear term partially implicitly in the equation for the fluid and evaluate the nonlinear term in the equation for the surfactant completely explicitly. The developed scheme is linear and decoupled, and the unconditional energy stability, the mass conservation, and the convergence are proved rigorously in the fully discrete setting. Various numerical experiments illustrate the stability and convergence of proposed scheme, along with the effectiveness in the long-time simulations.

Keywords: binary fluid-surfactant model, exponential time differencing scheme, linear convex splitting, unconditional energy stability, optimal error estimate

1. Introduction

Surfactant is an important organic compound that changes or reduces the surface tension of the solution and allows the immiscible liquid to mix. It is well known that the typical representatives of different liquids are oil and water, and water molecules are polar, which do not mix with chemical polarity such as oil. Therefore, in order to make the mixture more advantageous, a molecular intermediate, commonly known as surfactant, is required. Surfactant is such a group of amphiphilic molecules that bind water and oil molecules (the hydrophilic head enters the water and the hydrophobic tail into the oil) and mix the molecules by reducing the surface tension between the water and the oil. This is why people can use soap or detergent to clean their hands and clothes. In addition to the application in daily cleaning, surfactant has been widely used in industrial fields such as oil recovery and food processing.

There has been considerable research into the modeling and numerical simulation of binary fluid-surfactant system. In the pioneering work of Laradji et al. [21, 22], the phase transition behavior of single-layer microemulsions formed by surfactant molecules has been studied for the first time by using diffusion interface method, or phase field method. Since then, many phase field types of fluid-surfactant models have been developed, see, e.g., [7, 9, 30, 31]. In [20], Komura and Kodama established a novel model that contains two physical phase field variables, one for the local density of the fluid and the other for the local concentration of the surfactant. In addition to the regular potential (such as gradient entropy) and the hydrophobic part (nonlinear double well potential) of each phase field variable, there is a nonlinear coupling entropy term in the total free energy, accounting for the influence of the surfactant in boosting the formulation of interfaces.

Email addresses: 201921130055@mail.bnu.edu.cn (Yuzhuo Dong), xiao1li@polyu.edu.hk (Xiao Li), zqiao@polyu.edu.hk (Zhonghua Qiao), zrzhang@bnu.edu.cn (Zhengru Zhang)

By minimizing the total energy with the variation method, a control system consisting of two nonlinear coupled Cahn–Hilliard equations can be obtained.

For the numerical calculations, if the nonlinear terms are discretized in the conventional way, such as fully-implicit or explicit methods [6], some serious stability conditions require very small time steps, which leads to very high computational costs in practice. Therefore, it is necessary to establish an effective numerical scheme with better stability so that large time steps can be used. The energy stability is usually considered in designing numerical schemes for phase field models. A semi-implicit scheme was adopted in [30] with a small number of CFL conditions required. Gu et al. constructed an energy stable difference scheme for the binary fluid-surfactant system [10], based on the convex splitting method [5, 33], dealing implicitly with the convex part and explicitly with the concave part. The positivity preservation of the convex splitting scheme was analyzed in [27]. A variety of decouple and energy stable numerical schemes were proposed for the surfactant model by applying the invariant energy quadratization method [34, 35] and the scalar auxiliary variable approach [26, 36].

In recent years, the exponential time differencing (ETD) method [2, 14, 19] has been widely used in numerical simulations for phase field models [1, 3, 15, 16, 17, 18] because of the ability to provide a better temporal accuracy and preserve the exponential behavior of the linear part. In general, the linear part of the equation is integrated exactly and the nonlinear term is approximated explicitly by polynomial extrapolations. More details on stability analysis and applications of ETD schemes can be found in [3, 4, 8]. To the best of our knowledge, the ETD method has not ever been applied to the Cahn–Hilliard type binary fluid-surfactant system. We will make an initial exploration on this topic in this paper.

Our main contribution is to establish the first-order ETD scheme for the binary fluid-surfactant system and to give strict proofs of the unconditional energy stability and the optimal error estimates. In comparison with the existing numerical schemes mentioned above, the advantages of the established ETD scheme are embodied in three aspects. First, since there are high-order dissipation terms in the model (the sixth- and fourth-order terms in (2a) and (2b) given in the next section), the corresponding space-discrete problem will contain the highly stiff linear part. Due to the exact integration of the linear part, the ETD scheme preserves the exponential behavior of the linear operator, which leads to a better temporal accuracy for such problems with high stiffness. Second, the ETD scheme is linear and the coefficient matrices are given by some matrix exponentials, which can be implemented efficiently by, for instance, the fast Fourier transform we will adopt or the Krylov subspace methods for problems with irregular domains. Third, the scheme is energy stable with respect to the original energy rather than a modified form, so that the property of energy decay in practical problems is guaranteed theoretically. Unlike the explicit treatment of the nonlinear term in general, to guarantee the energy stability, we treat the nonlinear term partially implicitly in one equation (for the fluid) and evaluate the nonlinear term completely explicitly in the other equation (for the surfactant). As the numerical solutions of two unknown functions can be solved alternatively, the whole algorithm is still a linear and decoupled solver.

The organization of the paper is as follows. In Section 2, we briefly introduce the binary fluid-surfactant system established by Komura and Kodama. In Section 3, we establish the first-order ETD scheme to the phase field model of binary fluid-surfactant system. Section 4 is devoted to the analysis of the numerical scheme, including the energy stability and the optimal error estimates. In Section 5, we conduct numerical simulations to further validate the stability and convergence of the proposed scheme. Some numerical comparisons between the proposed ETD scheme and existing linear schemes are also given from the views of accuracy and efficiency. Finally, some concluding remarks are given in Section 6.

2. Phase field model of binary fluid-surfactant system

In the system of the mixture with water, oil and surfactant, the microemulsions can be formed as a random phase by monolayers of surfactant molecules. Usually, for the certain composition and temperature, the microphase separation occurs and various interesting microstructures can be observed in such microemulsion system. To simulate the dynamics of microphase separation, a common choice is the phase field approach with two phase field variables (order parameters). Here, we give a brief introduction of the binary fluid-surfactant phase field model presented in [20].

Let $\Omega = (0, X) \times (0, Y)$ be the physical domain, in which a phase field variable u is defined as a label for two fluids (such as water and oil), i.e.,

$$u = \begin{cases} 1, & \text{fluid I,} \\ -1, & \text{fluid II.} \end{cases}$$

The interface in the mixture can be described by the zero level set $\Gamma_t = \{\boldsymbol{x} \in \Omega \,|\, u(\boldsymbol{x}) = 0\}$. The other phase field variable ρ serves as the local concentration of surfactants. The free energy of the system is a functional with respect to u and ρ, given by

$$E(u, \rho) = \int_\Omega \Big\{ \underbrace{\frac{1}{2}|\nabla u|^2 + \frac{\alpha}{2}(\Delta u)^2 + \frac{1}{\epsilon^2}F(u)}_{\text{part A}} + \underbrace{\frac{\beta}{2}|\nabla \rho|^2 + \frac{1}{\eta^2}G(\rho)}_{\text{part B}} - \underbrace{\theta\rho|\nabla u|^2}_{\text{part C}} \Big\} \,\mathrm{d}\boldsymbol{x}, \tag{1}$$

where

$$F(u) = \frac{1}{4}(u^2 - 1)^2, \quad G(\rho) = \frac{1}{4}\rho^2(\rho - \rho_s)^2,$$

and α, β, ϵ, η, ρ_s, θ are all positive parameters. In part A, the first two terms describe the hydrophilic type of interactions between the fluids in the tendency of mixing, and the third term is the classic Ginzburg-Landau double-well potential corresponding to the hydrophobic type of interactions in the tendency of separation. The competition between these interactions results in a diffusion interface in the equilibrium configuration. In part B, the double-well potential for ρ enables two bulk states for the surfactant, i.e., $\rho = 0$ and $\rho = \rho_s$. The former represents that the local area is occupied by water and oil without surfactants, and the latter corresponds to the full occupation of surfactants. Here, ρ_s can be understood as the density of condensed hydrocarbon chains of surfactants, and we set $\rho_s = 1$ for simplicity. Taking into account of the feature of surfactants that altering the interfacial tension, the surfactant is expected to be clustered near the fluid interface, and this is described by the nonlinear coupling entropy between u and ρ in part C.

The evolution equations of u and ρ are established in the Cahn–Hilliard type, i.e., the gradient flow in H^{-1} of the energy (1). The system reads as

$$\begin{aligned} u_t &= M_u \Delta \mu_u, \\ \mu_u &= \frac{\delta E}{\delta u} = -\Delta u + \alpha \Delta^2 u + \frac{1}{\epsilon^2} f(u) + 2\theta \nabla \cdot (\rho \nabla u), \end{aligned} \tag{2a}$$

$$\begin{aligned} \rho_t &= M_\rho \Delta \mu_\rho, \\ \mu_\rho &= \frac{\delta E}{\delta \rho} = -\beta \Delta \rho + \frac{1}{\eta^2} g(\rho) - \theta |\nabla u|^2, \end{aligned} \tag{2b}$$

where $f(u) = F'(u)$, $g(\rho) = G'(\rho)$, and M_u and M_ρ are the mobility parameters. The periodic boundary conditions are equipped for both variables u and ρ in the system.

3. Exponential time differencing scheme

As we know [4], a suitable linear splitting can improve the stability of the numerical method. In this section, we establish a linear convex splitting of the energy. Then, we discretize the spatial domain and the time interval to design fully discrete numerical scheme for the model (2).

We first act some modifications on the potentials $F(u)$ and $G(\rho)$ to make their second derivatives bounded on the whole real line. For a given $\gamma_1 > 0$, we modify $F(u)$ by

$$\tilde{F}(u) = \begin{cases} \frac{3\gamma_1^2 - 1}{2}u^2 - 2\gamma_1^3 u + \frac{1}{4}(3\gamma_1^4 + 1), & u > \gamma_1, \\ \frac{1}{4}(u^2 - 1)^2, & u \in [-\gamma_1, \gamma_1], \\ \frac{3\gamma_1^2 - 1}{2}u^2 + 2\gamma_1^3 u + \frac{1}{4}(3\gamma_1^4 + 1), & u < -\gamma_1, \end{cases}$$

and replace $f(u)$ by $\tilde{F}'(u)$, that is,

$$\tilde{f}(u) = \tilde{F}'(u) = \begin{cases} (3\gamma_1^2 - 1)u - 2\gamma_1^3, & u > \gamma_1, \\ (u^2 - 1)u, & u \in [-\gamma_1, \gamma_1], \\ (3\gamma_1^2 - 1)u + 2\gamma_1^3, & u < -\gamma_1. \end{cases}$$

Then, we have $\max_{u\in\mathbb{R}} |\tilde{f}'(u)| \le 3\gamma_1^2 - 1$ and $\tilde{F}(u) \to F(u)$ pointwise as $\gamma_1 \to \infty$. Similarly, for a given $\gamma_2 > 0$, we modify $G(\rho)$ (with $\rho_s = 1$) by

$$\tilde{G}(\rho) = \begin{cases} (\frac{3}{2}\gamma_2^2 + \frac{3}{2}\gamma_2 + \frac{1}{4})\rho^2 - 2(1+\gamma_2)^3\rho + \frac{3}{2}(1+\gamma_2)^2\rho + \frac{3}{4}(1+\gamma_2)^4 - \frac{1}{2}(1+\gamma_2)^3, & \rho > 1+\gamma_2, \\ \frac{1}{4}\rho^2(\rho-1)^2, & \rho \in [-\gamma_2, 1+\gamma_2], \\ (\frac{3}{2}\gamma_2^2 + \frac{3}{2}\gamma_2 + \frac{1}{4})\rho^2 + 2\gamma_2^3\rho + \frac{3}{2}\gamma_2^2\rho + \frac{3}{4}\gamma_2^4 + \frac{1}{2}\gamma_2^3, & \rho < -\gamma_2, \end{cases}$$

and replace $g(\rho)$ by

$$\tilde{g}(\rho) = \tilde{G}'(\rho) = \begin{cases} (3\gamma_2^2 + 3\gamma_2 + \frac{1}{2})\rho - 2(1+\gamma_2)^3 + \frac{3}{2}(1+\gamma_2)^2, & \rho > 1+\gamma_2, \\ \rho^3 - \frac{3}{2}\rho^2 + \frac{1}{2}\rho, & \rho \in [-\gamma_2, 1+\gamma_2], \\ (3\gamma_2^2 + 3\gamma_2 + \frac{1}{2})\rho + 2\gamma_2^3 + \frac{3}{2}\gamma_2^2, & \rho < -\gamma_2. \end{cases}$$

Consequently, we have $\max_{\rho\in\mathbb{R}} |\tilde{g}'(\rho)| \le 3\gamma_2^2 + 3\gamma_2 + \frac{1}{2}$ and $\tilde{G}(\rho) \to G(\rho)$ pointwise when $\gamma_2 \to \infty$.

Remark 3.1. *To guarantee the uniform boundedness of the second derivative of the nonlinear potential, the regularization of the potential is a commonly-used technique in the numerical analysis for linear numerical schemes; see, e.g., [25, 29, 36]. Such a modification only changes the value of $F(u)$ when u is located out of the range $[-\gamma_1, \gamma_1]$. In other words, if we choose γ_1 larger than the supremum norm of u, the solution to the model with the regularized potential is actually equivalent to the original one. The case for $G(\rho)$ is quite similar. Though we will not justify the supremum norm of the numerical solutions in the later analysis, the upper bounds can be observed in practical computations. Therefore, we can choose γ_1 and γ_2 large enough so that the computed solutions are exactly the approximate solutions to the original model.*

In the following, we only consider the model with the regularized potentials $\tilde{F}(u)$ and $\tilde{G}(\rho)$. For simplicity of notations, we omit the $\tilde{}$ symbol.

3.1. Linear convex splitting

We design the following linear convex splitting of the energy (1) as $E(u,\rho) = E_c(u,\rho) - E_e(u,\rho)$ with

$$E_c(u,\rho) = \int_\Omega \Big(\frac{1}{2}|\nabla u|^2 + \frac{\alpha}{2}(\Delta u)^2 + \frac{\beta}{2}|\nabla\rho|^2 + \frac{\kappa_1}{2}u^2 + \frac{\kappa_2}{2}\rho^2\Big)\,\mathrm{d}\boldsymbol{x}$$

and

$$E_e(u,\rho) = \int_\Omega \Big(\theta\rho|\nabla u|^2 - \frac{1}{\epsilon^2}F(u) - \frac{1}{\eta^2}G(\rho) + \frac{\kappa_1}{2}u^2 + \frac{\kappa_2}{2}\rho^2\Big)\,\mathrm{d}\boldsymbol{x},$$

where κ_1 and κ_2 are positive numbers to be determined and expected to be as small as possible.

Lemma 3.1. *Suppose that $u, \rho : \Omega \to \mathbb{R}$ are periodic and sufficiently regular. Then $E_c(u,\rho)$ and $E_e(u,\rho)$ are both convex with respect to each variable when the other is fixed if*

$$\kappa_1 \ge \frac{3\gamma_1^2 - 1}{\epsilon^2} \quad \textit{and} \quad \kappa_2 \ge \frac{1}{\eta^2}\Big(3\gamma_2^2 + 3\gamma_2 + \frac{1}{2}\Big). \tag{3}$$

Proof. (i) If ρ keeps fixed, the energy $E_c(u,\rho)$ and $E_e(u,\rho)$ can be regarded as functionals only with respect to u. Let

$$e_c(u,u_x,u_y,u_{xx},u_{yy},\rho)=\frac{1}{2}|\nabla u|^2+\frac{\alpha}{2}(\Delta u)^2+\frac{\beta}{2}|\nabla\rho|^2+\frac{\kappa_1}{2}u^2+\frac{\kappa_2}{2}\rho^2, \tag{4}$$

$$e_e(u,u_x,u_y,u_{xx},u_{yy},\rho)=\theta\rho|\nabla u|^2-\frac{1}{\epsilon^2}F(u)-\frac{1}{\eta^2}G(\rho)+\frac{\kappa_1}{2}u^2+\frac{\kappa_2}{2}\rho^2, \tag{5}$$

where ρ is treated as a parameter. Both e_c and e_e are functions of five independent variables. Denote

$$e_c(\boldsymbol{u},\rho)\triangleq e_c(u,u_x,u_y,u_{xx},u_{yy},\rho),\quad e_e(\boldsymbol{u},\rho)\triangleq e_c(u,u_x,u_y,u_{xx},u_{yy},\rho)$$

where $\boldsymbol{u}=(u,u_x,u_y,u_{xx},u_{yy})\triangleq(u_1,u_2,u_3,u_4,u_5)$. Then

$$E_c(u,\rho)=\int_\Omega e_c(\boldsymbol{u},\rho)\,\mathrm{d}\boldsymbol{x},\quad E_e(u,\rho)=\int_\Omega e_e(\boldsymbol{u},\rho)\,\mathrm{d}\boldsymbol{x}.$$

From (4) and (5), it is easy to get

$$\begin{aligned}
&\partial^2_{u_1}e_c(u_1,u_2,u_3,u_4,u_5,\rho)=\kappa_1,\\
&\partial^2_{u_2}e_c(u_1,u_2,u_3,u_4,u_5,\rho)=1,\\
&\partial^2_{u_3}e_c(u_1,u_2,u_3,u_4,u_5,\rho)=1,\\
&\partial^2_{u_4}e_c(u_1,u_2,u_3,u_4,u_5,\rho)=\alpha,\\
&\partial^2_{u_5}e_c(u_1,u_2,u_3,u_4,u_5,\rho)=\alpha,\\
&\partial^2_{u_1}e_e(u_1,u_2,u_3,u_4,u_5,\rho)=-\frac{1}{\epsilon^2}f'(u)+\kappa_1,\\
&\partial^2_{u_2}e_e(u_1,u_2,u_3,u_4,u_5,\rho)=2\theta\rho,\\
&\partial^2_{u_3}e_e(u_1,u_2,u_3,u_4,u_5,\rho)=2\theta\rho.\\
&\partial^2_{u_4}e_e(u_1,u_2,u_3,u_4,u_5,\rho)=0,\\
&\partial^2_{u_5}e_e(u_1,u_2,u_3,u_4,u_5,\rho)=0.
\end{aligned}$$

Now we notice that α,ϵ,θ are all positive parameters, so e_c and e_e are both convex with respect to $\boldsymbol{u}$ if and only if

$$\begin{cases}\kappa_1\geq 0,\\ \kappa_1-\dfrac{1}{\epsilon^2}f'(u)\geq 0,\end{cases}$$

which is satisfied if

$$\kappa_1\geq\frac{3\gamma_1^2-1}{\epsilon^2}.$$

Then, according to the definition of convex function, we have the inequalities

$$e_c(\lambda\boldsymbol{u}+(1-\lambda)\boldsymbol{v},\rho)\leq\lambda e_c(\boldsymbol{u},\rho)+(1-\lambda)e_c(\boldsymbol{v},\rho) \tag{6}$$

and

$$e_e(\lambda\boldsymbol{u}+(1-\lambda)\boldsymbol{v},\rho)\leq\lambda e_e(\boldsymbol{u},\rho)+(1-\lambda)e_e(\boldsymbol{v},\rho), \tag{7}$$

for any $\lambda\in(0,1)$ and $\boldsymbol{u},\boldsymbol{v}\in\mathbb{R}^5$. Integrating both sides of (6) and (7) in Ω leads to

$$E_c(\lambda u+(1-\lambda)v,\rho)\leq\lambda E_c(u,\rho)+(1-\lambda)E_c(v,\rho)$$

and

$$E_e(\lambda u+(1-\lambda)v,\rho)\leq\lambda E_e(u,\rho)+(1-\lambda)E_e(v,\rho),$$

which indicates that E_c and E_e are convex with respect to u when ρ is fixed.

(ii) If u keeps fixed, the energy $E_c(u,\rho)$ and $E_e(u,\rho)$ can be regarded as functionals only with respect to ρ. Rewrite (4) and (5) as

$$e_c(u,\rho,\rho_x,\rho_y)=\frac{1}{2}|\nabla u|^2+\frac{\alpha}{2}(\Delta u)^2+\frac{\beta}{2}|\nabla\rho|^2+\frac{\kappa_1}{2}u^2+\frac{\kappa_2}{2}\rho^2 \tag{8}$$

and

$$e_e(u,\rho,\rho_x,\rho_y)=\theta\rho|\nabla u|^2-\frac{1}{\epsilon^2}F(u)-\frac{1}{\eta^2}G(\rho)+\frac{\kappa_1}{2}u^2+\frac{\kappa_2}{2}\rho^2, \tag{9}$$

where u is treated as a parameter. Both e_c and e_e are functions of three independent variables. Denote

$$e_c(u,\boldsymbol{\rho})\triangleq e_c(u,\rho,\rho_x,\rho_y),\quad e_e(u,\boldsymbol{\rho})\triangleq e_c(u,\rho,\rho_x,\rho_y)$$

where $\boldsymbol{\rho}=(\rho,\rho_x,\rho_y)\triangleq(\rho_1,\rho_2,\rho_3)$. Then

$$E_c(u,\rho)=\int_\Omega e_c(u,\boldsymbol{\rho})\,\mathrm{d}\boldsymbol{x},\quad E_e(u,\rho)=\int_\Omega e_e(u,\boldsymbol{\rho})\,\mathrm{d}\boldsymbol{x}.$$

From (8) and (9), we get

$$\begin{aligned}
&\partial^2_{\rho_1}e_c(u,\rho_1,\rho_2,\rho_3)=\kappa_2,\\
&\partial^2_{\rho_2}e_c(u,\rho_1,\rho_2,\rho_3)=\beta,\\
&\partial^2_{\rho_3}e_c(u,\rho_1,\rho_2,\rho_3)=\beta,\\
&\partial^2_{\rho_1}e_e(u,\rho_1,\rho_2,\rho_3)=-\frac{1}{\eta^2}g'(\rho)+\kappa_2,\\
&\partial^2_{\rho_2}e_e(u,\rho_1,\rho_2,\rho_3)=0,\\
&\partial^2_{\rho_3}e_e(u,\rho_1,\rho_2,\rho_3)=0.
\end{aligned}$$

Now we notice that β,η are all positive parameters, so $e_c(u,\boldsymbol{\rho})$ and $e_e(u,\boldsymbol{\rho})$ are both convex with respect to $\boldsymbol{\rho}$ if and only if

$$\begin{cases}\kappa_2\geq 0,\\ \kappa_2-\dfrac{1}{\eta^2}g'(\rho)\geq 0,\end{cases}$$

which is satisfied if

$$\kappa_2\geq\frac{1}{\eta^2}\Big(3\gamma_2^2+3\gamma_2+\frac{1}{2}\Big).$$

Then we have

$$e_c(u,\lambda\boldsymbol{\rho}+(1-\lambda)\boldsymbol{\tau})\leq\lambda e_c(u,\boldsymbol{\rho})+(1-\lambda)e_c(u,\boldsymbol{\tau}) \tag{10}$$

and

$$e_e(u,\lambda\boldsymbol{\rho}+(1-\lambda)\boldsymbol{\tau})\leq\lambda e_e(u,\boldsymbol{\rho})+(1-\lambda)e_e(u,\boldsymbol{\tau}), \tag{11}$$

for any $\lambda\in(0,1)$ and $\boldsymbol{\rho},\boldsymbol{\tau}\in\mathbb{R}^3$. Integrating both sides of (10) and (11) leads to

$$E_c(u,\lambda\rho+(1-\lambda)\tau)\leq\lambda E_c(u,\rho)+(1-\lambda)E_c(u,\tau)$$

and

$$E_e(u,\lambda\rho+(1-\lambda)\tau)\leq\lambda E_e(u,\rho)+(1-\lambda)E_e(u,\tau),$$

which implies that E_c and E_e are convex with respect to ρ when u is fixed. □

The above convex splitting of the energy (1) motivates us rewrite the system (2) as

$$u_t = -M_u\big(\Delta^2 - \alpha\Delta^3 - \kappa_1\Delta\big)u - M_u\Delta\Big(-\frac{1}{\epsilon^2}f(u) - 2\theta\nabla\cdot(\rho\nabla u) + \kappa_1 u\Big),$$
$$\rho_t = -M_\rho\big(\beta\Delta^2 - \kappa_2\Delta\big)\rho - M_\rho\Delta\Big(-\frac{1}{\eta^2}g(\rho) + \theta|\nabla u|^2 + \kappa_2\rho\Big),$$

or in a simpler form as

$$u_t = -Lu - f(u,\rho), \tag{12a}$$
$$\rho_t = -K\rho - g(u,\rho), \tag{12b}$$

where $L = M_u\big(\Delta^2 - \alpha\Delta^3 - \kappa_1\Delta\big)$ and $K = M_\rho\big(\beta\Delta^2 - \kappa_2\Delta\big)$ are linear operators.

3.2. Fourier pseudo-spectral approximation for spatial discretization

Let N_x and N_y be two even numbers and $h_x = X/N_x$ and $h_y = Y/N_y$ be the uniform mesh sizes in each dimension. The $N_x \times N_y$ mesh $\Omega_\mathcal{N}$ of the domain Ω is a collection of nodes (x_i, y_j) with $x_i = ih_x$, $y_j = jh_y$, $1 \le i \le N_x$, $1 \le j \le N_y$. Denote by $\mathcal{M}_\mathcal{N}$ all of the two-dimensional periodic grid functions defined on $\Omega_\mathcal{N}$, namely,

$$\mathcal{M}_\mathcal{N} = \{f : \mathbb{Z}^2 \to \mathbb{R} \,|\, f_{i+pN_x,j+qN_y} = f_{ij},\ \forall\,(p,q) \in \mathbb{Z}^2\}.$$

We define the index sets

$$J_\mathcal{N} = \{(i,j) \in \mathbb{Z}^2 \,|\, 1 \le i \le N_x,\ 1 \le j \le N_y\},$$
$$\widehat{J}_\mathcal{N} = \Big\{(k,l) \in \mathbb{Z}^2 \,\Big|\, -\frac{N_x}{2} + 1 \le k \le \frac{N_x}{2},\ -\frac{N_y}{2} + 1 \le l \le \frac{N_y}{2}\Big\}.$$

For a function $f \in \mathcal{M}_\mathcal{N}$, the two-dimensional discrete Fourier transform $\widehat{f} = Pf$ is defined componentwise [28, 32] by

$$\widehat{f}_{kl} = \frac{1}{N_xN_y}\sum_{(i,j)\in J_\mathcal{N}} f_{ij}\exp\left(-\mathrm{i}\frac{2k\pi}{X}x_i\right)\exp\left(-\mathrm{i}\frac{2l\pi}{Y}y_j\right), \quad (k,l) \in \widehat{J}_\mathcal{N}.$$

The function f can be reconstructed via the corresponding inverse transform $f = P^{-1}\widehat{f}$ with components given by

$$f_{ij} = \sum_{(k,l)\in\widehat{J}_\mathcal{N}} \widehat{f}_{kl}\exp\left(\mathrm{i}\frac{2k\pi}{X}x_i\right)\exp\left(\mathrm{i}\frac{2l\pi}{Y}y_j\right), \quad (i,j) \in J_\mathcal{N}.$$

Let $\widehat{\mathcal{M}}_\mathcal{N} = \{Pf \,|\, f \in \mathcal{M}_\mathcal{N}\}$ and define the operators $\widehat{D}_x$ and $\widehat{D}_y$ on $\widehat{\mathcal{M}}_\mathcal{N}$ as

$$(\widehat{D}_x\widehat{f})_{kl} = \left(\frac{2k\pi\mathrm{i}}{X}\right)\widehat{f}_{kl}, \quad (\widehat{D}_y\widehat{f})_{kl} = \left(\frac{2k\pi\mathrm{i}}{Y}\right)\widehat{f}_{kl}, \quad (k,l) \in \widehat{J}_\mathcal{N}.$$

The Fourier pseudo-spectral approximations of the first- and second-order partial derivatives can be represented as

$$D_x = P^{-1}\widehat{D}_xP, \quad D_y = P^{-1}\widehat{D}_yP, \qquad D_x^2 = P^{-1}\widehat{D}_x^2P, \quad D_y^2 = P^{-1}\widehat{D}_y^2P.$$

For any $f, g \in \mathcal{M}_\mathcal{N}$ and $\boldsymbol{f} = (f_1, f_2)^T, \boldsymbol{g} = (g_1, g_2)^T \in \mathcal{M}_\mathcal{N} \times \mathcal{M}_\mathcal{N}$, the discrete gradient, divergence and Laplace operators are given, respectively, by

$$\nabla_\mathcal{N} f = \begin{pmatrix} D_xf \\ D_yf \end{pmatrix}, \quad \nabla_\mathcal{N}\cdot\boldsymbol{f} = D_xf^1 + D_yf^2, \quad \Delta_\mathcal{N} f = D_x^2f + D_y^2f,$$

and the discrete L^2 inner product $(\cdot,\cdot)_\mathcal{N}$, the discrete L^2 norm $\|\cdot\|_\mathcal{N}$, and the discrete L^∞ norm $\|\cdot\|_\infty$ by

$$(f,g)_\mathcal{N} = h_xh_y\sum_{(i,j)\in J_\mathcal{N}} f_{ij}g_{ij}, \quad \|f\|_\mathcal{N} = \sqrt{(f,f)_\mathcal{N}}, \quad \|f\|_\infty = \max_{(i,j)\in J_\mathcal{N}}|f_{ij}|,$$

$$(\boldsymbol{f},\boldsymbol{g})_{\mathcal{N}} = h_x h_y \sum_{(i,j)\in J_{\mathcal{N}}} (f_{ij}^1 g_{ij}^1 + f_{ij}^2 g_{ij}^2), \quad \|\boldsymbol{f}\|_{\mathcal{N}} = \sqrt{(\boldsymbol{f},\boldsymbol{f})_{\mathcal{N}}}, \quad \|\boldsymbol{f}\|_{\infty} = \max_{(i,j)\in J_{\mathcal{N}}} \sqrt{|f_{ij}^1|^2 + |f_{ij}^2|^2}.$$

Define a subspace of $\mathcal{M}_{\mathcal{N}}$ by $\mathcal{M}_{\mathcal{N}}^0 = \{f \in \mathcal{M}_{\mathcal{N}} \,|\, (f,1)_{\mathcal{N}} = 0\}$.

Proposition 3.2. *For any functions $f, g \in \mathcal{M}_{\mathcal{N}}$ and $\boldsymbol{g} \in \mathcal{M}_{\mathcal{N}} \times \mathcal{M}_{\mathcal{N}}$, we have the discrete integration-by-parts formulas*

$$(f, \nabla_{\mathcal{N}} \cdot \boldsymbol{g})_{\mathcal{N}} = -(\nabla_{\mathcal{N}} f, \boldsymbol{g})_{\mathcal{N}}, \quad (f, \Delta_{\mathcal{N}} g)_{\mathcal{N}} = -(\nabla_{\mathcal{N}} f, \nabla_{\mathcal{N}} g)_{\mathcal{N}} = (\Delta_{\mathcal{N}} f, g)_{\mathcal{N}}$$

By Proposition 3.2, the linear operator $L_{\mathcal{N}} = M_u\big(\Delta_{\mathcal{N}}^2 - \alpha\Delta_{\mathcal{N}}^3 - \kappa_1\Delta_{\mathcal{N}}\big)$ is symmetric on $\mathcal{M}_{\mathcal{N}}$, i.e., $(L_{\mathcal{N}}u, v)_{\mathcal{N}} = (u, L_{\mathcal{N}}v)_{\mathcal{N}}$ for any $u, v \in \mathcal{M}_{\mathcal{N}}$. Moreover, for any $u \in \mathcal{M}_{\mathcal{N}}$, we have

$$(L_{\mathcal{N}}u, u)_{\mathcal{N}} = M_u\|\Delta_{\mathcal{N}}u\|_{\mathcal{N}}^2 + M_u\alpha\|\Delta_{\mathcal{N}}\nabla_{\mathcal{N}}u\|_{\mathcal{N}}^2 + M_u\kappa_1\|\nabla_{\mathcal{N}}u\|_{\mathcal{N}}^2 \geq 0,$$

which means that $L_{\mathcal{N}}$ is symmetric and nonnegative definite. Moreover, $L_{\mathcal{N}}$ is positive definite, and thus invertible, on $\mathcal{M}_{\mathcal{N}}^0$. Similarly, $K_{\mathcal{N}}$ is positive definite on $\mathcal{M}_{\mathcal{N}}^0$.

The space-discrete scheme for the system (12) is to find functions $\widetilde{u} : [0,T] \to \mathcal{M}_{\mathcal{N}}$ and $\widetilde{\rho} : [0,T] \to \mathcal{M}_{\mathcal{N}}$ such that

$$\frac{\mathrm{d}\widetilde{u}}{\mathrm{d}t} = -L_{\mathcal{N}}\widetilde{u} - f_{\mathcal{N}}(\widetilde{u},\widetilde{\rho}), \tag{13a}$$

$$\frac{\mathrm{d}\widetilde{\rho}}{\mathrm{d}t} = -K_{\mathcal{N}}\widetilde{\rho} - g_{\mathcal{N}}(\widetilde{u},\widetilde{\rho}), \tag{13b}$$

where $L_{\mathcal{N}}$, $K_{\mathcal{N}}$, $f_{\mathcal{N}}$ and $g_{\mathcal{N}}$ correspond to the discrete forms of L, K, f and g, respectively.

3.3. Fully discrete ETD scheme for the binary fluid-surfactant system

We first present the following lemma, which is the basis of the establishment, analysis, and implementation of the fully discrete ETD scheme.

Lemma 3.3 ([13])**.** *Let f be defined on the spectrum of $M \in \mathbb{C}^{d\times d}$, that is, the values*

$$f^{(j)}(\lambda_i), \qquad 0 \leq j \leq n_i - 1, \quad 1 \leq i \leq d,$$

exist, where $\{\lambda_i\}_{i=1}^d$ are the eigenvalues of M, and n_i is the order of the largest Jordan block where λ_i appears. Then

(1) *$f(M)$ commutes with M;*
(2) *$f(M^T) = f(M)^T$;*
(3) *the eigenvalues of $f(M)$ are $f(\lambda_i), 1 \leq i \leq d$;*
(4) *$f(P^{-1}MP) = P^{-1}f(M)P$ for any nonsingular matrix $P \in \mathbb{C}^{d\times d}$.*

To establish the fully discrete ETD schemes for the binary fluid-surfactant model, let us focus on the space-discrete system (13a) as example, and the deduction for (13b) is completely similar.

Acting the operator $\mathrm{e}^{L_{\mathcal{N}}t}$ on both sides of (13a) leads to

$$\frac{\mathrm{d}(\mathrm{e}^{L_{\mathcal{N}}t}\widetilde{u})}{\mathrm{d}t} = -\mathrm{e}^{L_{\mathcal{N}}t} f_{\mathcal{N}}(\widetilde{u},\widetilde{\rho}),$$

where $\mathrm{e}^{L_{\mathcal{N}}t} = \sum_{k=0}^{\infty} \frac{1}{k!}(tL_{\mathcal{N}})^k$. Given a time step $\Delta t > 0$, we use the nodes $\{t_n = n\Delta t\}_{n\geq 0}$ to partition the time interval. Integrating the above equation from t_n to t_{n+1} yields

$$\widetilde{u}(t_{n+1}) = \mathrm{e}^{-L_{\mathcal{N}}\Delta t}\widetilde{u}(t_n) - \int_0^{\Delta t} \mathrm{e}^{-L_{\mathcal{N}}(\Delta t-\tau)} \widetilde{f}_{\mathcal{N}}(t_n+\tau)\,\mathrm{d}\tau, \tag{14}$$

where $\widetilde{f}_{\mathcal{N}}(t) = f_{\mathcal{N}}(\widetilde{u}(t), \widetilde{\rho}(t))$. Then, we approximate $\widetilde{f}_{\mathcal{N}}(t_n + \tau)$ by using the Lagrange polynomial interpolation of degree r based on the nodes $t_n, t_{n-1}, \ldots, t_{n-r}$ as follows:

$$\widetilde{f}_{\mathcal{N}}(t_n + \tau) \approx \sum_{s=0}^{r} \prod_{q=0, q\neq s}^{r} \frac{t - t_{n-q}}{t_{n-s} - t_{n-q}} \cdot \widetilde{f}_{\mathcal{N}}(t_{n-s}) = \sum_{s=0}^{r} \ell_{r,s}\Big(\frac{\tau}{\Delta t}\Big) \widetilde{f}_{\mathcal{N}}(t_{n-s}),$$

where $\ell_{r,s}(\xi) = \displaystyle\prod_{q=0, q\neq s}^{r} \frac{q + \xi}{q - s}$ is the basis function of the Lagrange interpolation. The integral in (14) can be approximated by

$$\int_0^{\Delta t} \mathrm{e}^{-L_{\mathcal{N}}(\Delta t - \tau)} \widetilde{f}_{\mathcal{N}}(t_n + \tau)\, \mathrm{d}\tau \approx \Delta t \sum_{s=0}^{r} S_{r,s}(-L_{\mathcal{N}}\Delta t) \widetilde{f}_{\mathcal{N}}(t_{n-s}),$$

where

$$S_{r,s}(a) = \frac{1}{\Delta t} \int_0^{\Delta t} \ell_{r,s}\Big(\frac{\tau}{\Delta t}\Big) \mathrm{e}^{a(1 - \frac{\tau}{\Delta t})}\, \mathrm{d}\tau = \int_0^1 \ell_{r,s}(\xi) \mathrm{e}^{a(1-\xi)}\, \mathrm{d}\xi, \quad a \in \mathbb{R}.$$

Then the ETD multistep scheme for solving (13a) reads as

$$u^{n+1} = \mathrm{e}^{-L_{\mathcal{N}}\Delta t} u^n - \Delta t \sum_{s=0}^{r} S_{r,s}(-L_{\mathcal{N}}\Delta t) f_{\mathcal{N}}(u^{n-s}, \rho^{n-s}).$$

The operator $S_{r,s}(-L_{\mathcal{N}}\Delta t)$ does not depend on time in the case of uniform time partition.

In particular, for the cases $r = 0$ and $r = 1$, we have

$$\ell_{0,0}(\xi) = 1, \quad \ell_{1,0}(\xi) = 1 + \xi, \quad \ell_{1,1}(\xi) = -\xi,$$

and correspondingly,

$$S_{0,0}(a) = \phi_1(a), \quad S_{1,0}(a) = \phi_1(a) + \phi_2(a), \quad S_{1,1}(a) = -\phi_2(a),$$

where

$$\begin{cases} \phi_1(a) = \dfrac{\mathrm{e}^a - 1}{a},\ \phi_{p+1}(a) = \dfrac{p\phi_p(a) - 1}{a}, & a \neq 0, \\ \phi_p(a) = \dfrac{1}{p}, & a = 0. \end{cases}$$

The case $r = 0$ leads to the first-order ETD scheme

$$u^{n+1} = \phi_0(-L_{\mathcal{N}}\Delta t) u^n - \Delta t \phi_1(-L_{\mathcal{N}}\Delta t) f_{\mathcal{N}}(u^n, \rho^n), \tag{15}$$

and the case $r = 1$ yields the second-order ETD multistep scheme

$$u^{n+1} = \phi_0(-L_{\mathcal{N}}\Delta t) u^n - \Delta t \phi_1(-L_{\mathcal{N}}\Delta t) f_{\mathcal{N}}(u^n, \rho^n) - \Delta t \phi_2(-L_{\mathcal{N}}\Delta t)[f_{\mathcal{N}}(u^n, \rho^n) - f_{\mathcal{N}}(u^{n-1}, \rho^{n-1})]. \tag{16}$$

where we denote $\phi_0(a) = \mathrm{e}^a$.

In this paper, we only focus on the first-order scheme. For the sake of the energy stability, we slightly modify the formulation (15) and establish the first-order ETD (ETD1) scheme for the binary fluid-surfactant model (2) as follows:

$$u^{n+1} = \phi_0(-L_{\mathcal{N}}\Delta t) u^n - \Delta t \phi_1(-L_{\mathcal{N}}\Delta t) f_{\mathcal{N}}(u^n, \rho^{n+1}), \tag{17a}$$

$$\rho^{n+1} = \phi_0(-K_{\mathcal{N}}\Delta t) \rho^n - \Delta t \phi_1(-K_{\mathcal{N}}\Delta t) g_{\mathcal{N}}(u^n, \rho^n). \tag{17b}$$

We remark that the ETD1 scheme (17) is well defined. In fact, for any $v \in \mathcal{M}_{\mathcal{N}}$, we know $(\Delta_{\mathcal{N}} v, 1)_{\mathcal{N}} = 0$, which means $\Delta_{\mathcal{N}} v \in \mathcal{M}_{\mathcal{N}}^0$. By the definition of $f_{\mathcal{N}}$, the term $f_{\mathcal{N}}(u^n, \rho^{n+1})$ must be in $\mathcal{M}_{\mathcal{N}}^0$, so that the action of $\phi_1(-L_{\mathcal{N}}\Delta t) = (L_{\mathcal{N}}\Delta t)^{-1}(I - \mathrm{e}^{-L_{\mathcal{N}}\Delta t})$ on $f_{\mathcal{N}}(u^n, \rho^{n+1})$ makes sense. Therefore, u^{n+1} is well defined by (17a). Similar explanations are suitable for (17b).

Due to the variation structure inheriting from the continuous model, the ETD1 scheme satisfies the mass conservation in the discrete setting. We present the following proposition without proof as it is in the similar spirit to that provided in [15].

Proposition 3.4. *The solution (u^n, ρ^n) defined by the ETD1 scheme* (17) *satisfies the discrete mass conservation, i.e., $(u^{n+1}, 1)_{\mathcal{N}} = (u^n, 1)_{\mathcal{N}}$ and $(\rho^{n+1}, 1)_{\mathcal{N}} = (\rho^n, 1)_{\mathcal{N}}$.*

To close this section, we give a brief illustration on the implementation of the numerical scheme established here. The nonlinear term $f_{\mathcal{N}}(u^n, \rho^{n+1})$ in (17a) involves the unknown solution ρ^{n+1} for the sake of the energy stability, so one needs to calculate ρ^{n+1} first from (17b) and then solve u^{n+1} from (17a). The main computational cost comes from the actions of the operator functions $\phi_i(-L_{\mathcal{N}}\Delta t)$ and $\phi_i(-K_{\mathcal{N}}\Delta t)$, $i = 0, 1$, which can be implemented via the fast Fourier transform (FFT) due to the periodic boundary condition. More precisely, let us recall the linear operator $L_{\mathcal{N}}$ defined as

$$\begin{aligned} L_{\mathcal{N}} &= M_u\big((D_x^2 + D_y^2)^2 - \alpha(D_x^2 + D_y^2)^3 - \kappa(D_x^2 + D_y^2)\big) \\ &= M_u P^{-1}\big((\widehat{D}_x^2 + \widehat{D}_y^2)^2 - \alpha(\widehat{D}_x^2 + \widehat{D}_y^2)^3 - \kappa_1(\widehat{D}_x^2 + \widehat{D}_y^2)\big)P = P^{-1}\widehat{L}_{\mathcal{N}}P, \end{aligned}$$

where the operator $\widehat{L}_{\mathcal{N}} = M_u((\widehat{D}_x^2 + \widehat{D}_y^2)^2 - \alpha(\widehat{D}_x^2 + \widehat{D}_y^2)^3 - \kappa_1(\widehat{D}_x^2 + \widehat{D}_y^2))$ can be expressed as

$$(\widehat{L}_{\mathcal{N}}\widehat{f})_{kl} = M_u\lambda_{kl}\widehat{f}_{kl}, \quad (k,l) \in \widehat{J}_{\mathcal{N}},$$

for any $\widehat{f} \in \widehat{\mathcal{M}}_{\mathcal{N}}$, where $\{\lambda_{kl} \,|\, (k,l) \in \widehat{J}_{\mathcal{N}}\}$ are the eigenvalues of $M_u^{-1}\widehat{L}_{\mathcal{N}}$, that is,

$$\lambda_{kl} = \left(\frac{4k^2\pi^2}{X^2} + \frac{4l^2\pi^2}{Y^2}\right)^2 + \alpha\left(\frac{4k^2\pi^2}{X^2} + \frac{4l^2\pi^2}{Y^2}\right)^3 + \kappa_1\left(\frac{4k^2\pi^2}{X^2} + \frac{4l^2\pi^2}{Y^2}\right).$$

Similarly,

$$\begin{aligned} K_{\mathcal{N}} &= M_\rho\big(\beta(D_x^2 + D_y^2)^2 - \kappa_2(D_x^2 + D_y^2)\big) \\ &= M_\rho P^{-1}\big(\beta(\widehat{D}_x^2 + \widehat{D}_y^2)^2 - \kappa_2(\widehat{D}_x^2 + \widehat{D}_y^2)\big)P = P^{-1}\widehat{K}_{\mathcal{N}}P, \end{aligned}$$

where $\widehat{K}_{\mathcal{N}} = M_\rho(\beta(\widehat{D}_x^2 + \widehat{D}_y^2)^2 - \kappa_2(\widehat{D}_x^2 + \widehat{D}_y^2))$ can be expressed as

$$(\widehat{K}_{\mathcal{N}}\widehat{f})_{kl} = M_\rho\mu_{kl}\widehat{f}_{kl}, \quad (k,l) \in \widehat{J}_{\mathcal{N}}$$

for any $\widehat{f} \in \widehat{\mathcal{M}}_{\mathcal{N}}$, where $\{\mu_{kl} \,|\, (k,l) \in \widehat{J}_{\mathcal{N}}\}$ are the eigenvalues of $M_\rho^{-1}\widehat{K}_{\mathcal{N}}$, that is,

$$\mu_{kl} = \beta\left(\frac{4k^2\pi^2}{X^2} + \frac{4l^2\pi^2}{Y^2}\right)^2 + \kappa_2\left(\frac{4k^2\pi^2}{X^2} + \frac{4l^2\pi^2}{Y^2}\right).$$

Then, the ETD1 scheme (17) can be implemented via the following formulas:

$$\begin{aligned} u^{n+1} &= P^{-1}[\phi_0(-\widehat{L}_{\mathcal{N}}\Delta t)Pu^n - \Delta t\phi_1(-\widehat{L}_{\mathcal{N}}\Delta t)Pf_{\mathcal{N}}(u^n, \rho^{n+1})], \\ \rho^{n+1} &= P^{-1}[\phi_0(-\widehat{K}_{\mathcal{N}}\Delta t)P\rho^n - \Delta t\phi_1(-\widehat{K}_{\mathcal{N}}\Delta t)Pg_{\mathcal{N}}(u^n, \rho^n)], \end{aligned}$$

where P and P^{-1} correspond to the FFT and its inverse transform, and

$$(\phi_i(-\widehat{L}_{\mathcal{N}}\Delta t)\widehat{f})_{kl} = \phi_i(-M_u\lambda_{kl}\Delta t)\widehat{f}_{kl}, \quad (\phi_i(-\widehat{K}_{\mathcal{N}}\Delta t)\widehat{f})_{kl} = \phi_i(-M_\rho\mu_{kl}\Delta t)\widehat{f}_{kl}, \quad i = 0, 1,$$

for any $\widehat{f} \in \widehat{\mathcal{M}}_{\mathcal{N}}$ and $(k,l) \in \widehat{J}_{\mathcal{N}}$.

Remark 3.2. *As the periodic boundary condition is applied to the model* (2)*, the Fourier spectral approximation is a natural choice for the spatial discretization. For the ETD1 scheme* (17)*, although we only have a first-order accuracy in time, the spatial spectral accuracy allows us to obtain highly accurate results by using fewer mesh nodes than those required for some lower-order spatial discretizations, such as the finite difference and finite element methods. Meanwhile, the Fourier transform can be implemented by the fast algorithm, so that the fully discrete ETD1 scheme* (17) *is adequate to the practical numerical simulations. In addition to the periodic boundary conditions, the homogeneous Neumann boundary condition is also usually considered as a type of physical boundary conditions. For this case, one can apply the spectral method based on the Chebyshev polynomials to match the boundary condition, and the corresponding Chebyshev transform can also be implemented by appropriate fast approaches based on the FFT. For the sake of the simplicity of the discussions and the lengthiness of this paper, we only focus on the numerical analysis and simulations for the case of the periodic boundary condition.*

4. Energy stability and convergence analysis

This section is devoted to the theoretical analysis of the energy stability and convergence of the proposed ETD1 scheme (17). In the rest of the paper, we always suppose κ_1 and κ_2 satisfy (3).

4.1. Unconditional energy stability

Recalling the definition of $\Delta_{\mathcal{N}}$ and Proposition 3.2, we know that $-\Delta_{\mathcal{N}}$ is symmetric and positive definite, and thus invertible, on $\mathcal{M}_{\mathcal{N}}^0$. Denote by $(-\Delta_{\mathcal{N}})^{-1}$ the inverse of $-\Delta_{\mathcal{N}}$ on $\mathcal{M}_{\mathcal{N}}^0$, so $(-\Delta_{\mathcal{N}})^{-1}$ is also symmetric and positive definite.

The energy functional at the discrete level corresponding to the continuous one $E(u,\rho)$ can be defined as

$$E_{\mathcal{N}}(u,\rho)=\Big(\frac{1}{\epsilon^2}F(u)+\frac{1}{\eta^2}G(\rho)-\theta\rho|\nabla_{\mathcal{N}}u|^2,1\Big)_{\mathcal{N}}+\frac{1}{2}\|\nabla_{\mathcal{N}}u\|_{\mathcal{N}}^2+\frac{\alpha}{2}\|\Delta_{\mathcal{N}}u\|_{\mathcal{N}}^2+\frac{\beta}{2}\|\nabla_{\mathcal{N}}\rho\|_{\mathcal{N}}^2. \tag{18}$$

Also we define the following discrete convex parts corresponding to E_c and E_e as

$$E_{\mathcal{N},c}=\frac{1}{2}\|\nabla_{\mathcal{N}}u\|_{\mathcal{N}}^2+\frac{\alpha}{2}\|\Delta_{\mathcal{N}}u\|_{\mathcal{N}}^2+\frac{\beta}{2}\|\nabla_{\mathcal{N}}\rho\|_{\mathcal{N}}^2+\frac{\kappa_1}{2}\|u\|_{\mathcal{N}}^2+\frac{\kappa_2}{2}\|\rho\|_{\mathcal{N}}^2$$

and

$$E_{\mathcal{N},e}=-\Big(\frac{1}{\epsilon^2}F(u)+\frac{1}{\eta^2}G(\rho)-\theta\rho|\nabla_{\mathcal{N}}u|^2,1\Big)_{\mathcal{N}}+\frac{\kappa_1}{2}\|u\|_{\mathcal{N}}^2+\frac{\kappa_2}{2}\|\rho\|_{\mathcal{N}}^2.$$

Based on the convex splitting form $E_{\mathcal{N}}=E_{\mathcal{N},c}-E_{\mathcal{N},e}$, we have the following lemma.

Lemma 4.1. *Suppose that $u,v,\rho,\tau:\Omega_{\mathcal{N}}\to\mathbb{R}$ are periodic and sufficiently regular. Considering the discrete energy $E_{\mathcal{N}}(u,\rho)$ in (18), we have*

(i) $E_{\mathcal{N}}(u,\rho)-E_{\mathcal{N}}(v,\rho)\le\big((-\Delta_{\mathcal{N}})^{-1}L_{\mathcal{N}}u+(-\Delta_{\mathcal{N}})^{-1}f_{\mathcal{N}}(v,\rho),u-v\big)_{\mathcal{N}}$;

(ii) $E_{\mathcal{N}}(u,\rho)-E_{\mathcal{N}}(u,\tau)\le\big((-\Delta_{\mathcal{N}})^{-1}K_{\mathcal{N}}u+(-\Delta_{\mathcal{N}})^{-1}g_{\mathcal{N}}(u,\tau),\rho-\tau\big)_{\mathcal{N}}$.

Proof. Define a continuously differentiable function in $\mathbb{R}$ as $j_c(s)=E_{\mathcal{N},c}(u+sv,\rho)$. With the convexity of $E_{\mathcal{N},c}$, we get the convexity of $j_c(s)$ in $\mathbb{R}$, so $j_c(1)-j_c(0)\ge j_c'(0)(1-0)$, i.e.,

$$E_{\mathcal{N},c}(u+v,\rho)-E_{\mathcal{N},c}(u,\rho)\ge(\delta_uE_{\mathcal{N},c}(u,\rho),v)_{\mathcal{N}}.$$

Replacing v by $v-u$ leads to

$$E_{\mathcal{N},c}(v,\rho)-E_{\mathcal{N},c}(u,\rho)\ge(\delta_uE_{\mathcal{N},c}(u,\rho),v-u)_{\mathcal{N}}. \tag{19}$$

Repeating the deduction above on $E_{\mathcal{N},e}$ and exchanging u and v lead to

$$E_{\mathcal{N},e}(u,\rho)-E_{\mathcal{N},e}(v,\rho)\ge(\delta_uE_{\mathcal{N},e}(v,\rho),u-v)_{\mathcal{N}}. \tag{20}$$

Adding the inequalities (19) and (20), we have

$$E_{\mathcal{N}}(u,\rho)-E_{\mathcal{N}}(v,\rho)\le(\delta_uE_{\mathcal{N},c}(u,\rho)-\delta_uE_{\mathcal{N},e}(v,\rho),u-v)_{\mathcal{N}}.$$

Some direct computations give us

$$\delta_uE_{\mathcal{N},c}(u,\rho)=(-\Delta_{\mathcal{N}})^{-1}L_{\mathcal{N}}u,\quad\delta_uE_{\mathcal{N},e}(v,\rho)=-(-\Delta_{\mathcal{N}})^{-1}f_{\mathcal{N}}(v,\rho),$$

which leads to the expected inequality in (i).

Similar to the above procedure, by considering the function $k_c(s)=E_{\mathcal{N},c}(u,\rho+s\tau)$ and noting that

$$\delta_\rho E_{\mathcal{N},c}(u,\rho)=(-\Delta_{\mathcal{N}})^{-1}K_{\mathcal{N}}u,\quad\delta_\rho E_{\mathcal{N},e}(u,\tau)=-(-\Delta_{\mathcal{N}})^{-1}g_{\mathcal{N}}(u,\tau),$$

we can obtain the inequality in (ii). □

Theorem 4.2. *The solution to the ETD1 scheme* (17) *satisfies the energy inequality*

$$E_{\mathcal{N}}(u^{n+1},\rho^{n+1}) \le E_{\mathcal{N}}(u^n,\rho^n)$$

for any time step size $\Delta t>0$*, i.e., the ETD1 scheme* (17) *is unconditionally energy stable.*

Proof. Reformulate the ETD1 scheme (17) as follows:

$$u^{n+1} = \mathrm{e}^{-L_{\mathcal{N}}\Delta t}u^n - L_{\mathcal{N}}^{-1}(I-\mathrm{e}^{-L_{\mathcal{N}}\Delta t})f_{\mathcal{N}}(u^n,\rho^{n+1}), \tag{21a}$$

$$\rho^{n+1} = \mathrm{e}^{-K_{\mathcal{N}}\Delta t}\rho^n - K_{\mathcal{N}}^{-1}(I-\mathrm{e}^{-K_{\mathcal{N}}\Delta t})g_{\mathcal{N}}(u^n,\rho^n). \tag{21b}$$

Now we define $\sigma_1(a)=1-\mathrm{e}^{-a\Delta t}$ for $a\in\mathbb{R}$ and an operator $B_1=\sigma_1(L_{\mathcal{N}})=I-\mathrm{e}^{-L_{\mathcal{N}}\Delta t}$. Noting that $0<\sigma_1(a)<1$ for any $a>0$ and $L_{\mathcal{N}}$ is symmetric positive, we know from Lemma 3.3 that B_1 is also symmetric positive definite and commutes with $L_{\mathcal{N}}$. Thus we have from (21a) that

$$\begin{aligned} f_{\mathcal{N}}(u^n,\rho^{n+1}) &= -B_1^{-1}L_{\mathcal{N}}(u^{n+1}-\mathrm{e}^{-L_{\mathcal{N}}\Delta t}u^n)\\ &= -B_1^{-1}L_{\mathcal{N}}(u^{n+1}-u^n+(I-\mathrm{e}^{-L_{\mathcal{N}}\Delta t})u^n)\\ &= -B_1^{-1}L_{\mathcal{N}}(u^{n+1}-u^n)-L_{\mathcal{N}}u^n. \end{aligned}$$

By Lemma 4.1 (i), we have

$$\begin{aligned} &E_{\mathcal{N}}(u^{n+1},\rho^{n+1})-E_{\mathcal{N}}(u^n,\rho^{n+1})\\ &\quad\le ((-\Delta_{\mathcal{N}})^{-1}L_{\mathcal{N}}u^{n+1}+(-\Delta_{\mathcal{N}})^{-1}f_{\mathcal{N}}(u^n,\rho^{n+1}),u^{n+1}-u^n)_{\mathcal{N}}\\ &\quad= (L_{\mathcal{N}}u^{n+1}+f_{\mathcal{N}}(u^n,\rho^{n+1}),(-\Delta_{\mathcal{N}})^{-1}(u^{n+1}-u^n))_{\mathcal{N}}\\ &\quad= (L_{\mathcal{N}}u^{n+1}-B_1^{-1}L_{\mathcal{N}}(u^{n+1}-u^n)-L_{\mathcal{N}}u^n,(-\Delta_{\mathcal{N}})^{-1}(u^{n+1}-u^n))_{\mathcal{N}}\\ &\quad= (-B_1^{-1}L_{\mathcal{N}}(u^{n+1}-u^n)+L_{\mathcal{N}}(u^{n+1}-u^n),(-\Delta_{\mathcal{N}})^{-1}(u^{n+1}-u^n))_{\mathcal{N}}\\ &\quad= -(B_2(u^{n+1}-u^n),(-\Delta_{\mathcal{N}})^{-1}(u^{n+1}-u^n))_{\mathcal{N}}, \end{aligned}$$

where $B_2=\sigma_2(L_{\mathcal{N}})=(B_1^{-1}-I)L_{\mathcal{N}}$ with $\sigma_2(a):=\big(\frac{1}{\sigma_1(a)}-1\big)a$ for $a\neq 0$. For any $a>0$, we have $0<\sigma_1(a)<1$ and thus $\sigma_2(a)>0$, so that B_2 is symmetric and positive definite. Note that B_2 computes with $(-\Delta_{\mathcal{N}})^{-1}$, so we can obtain

$$E_{\mathcal{N}}(u^{n+1},\rho^{n+1})-E_{\mathcal{N}}(u^n,\rho^{n+1}) \le -((-\Delta_{\mathcal{N}})^{-1}B_2(u^{n+1}-u^n),u^{n+1}-u^n)_{\mathcal{N}} \le 0. \tag{22}$$

Similarly, define $D_1=\sigma_1(K_{\mathcal{N}})$ and $D_2=\sigma_2(K_{\mathcal{N}})$, then we have from (21b) that

$$g_{\mathcal{N}}(u^n,\rho^n) = -D_1^{-1}K_{\mathcal{N}}(\rho^{n+1}-\rho^n)-K_{\mathcal{N}}\rho^n,$$

and, by Lemma 4.1 (ii),

$$\begin{aligned} E_{\mathcal{N}}(u^n,\rho^{n+1})-E_{\mathcal{N}}(u^n,\rho^n) &\le ((-\Delta_{\mathcal{N}})^{-1}K_{\mathcal{N}}\rho^{n+1}+(-\Delta_{\mathcal{N}})^{-1}g_{\mathcal{N}}(u^n,\rho^n),\rho^{n+1}-\rho^n)_{\mathcal{N}}\\ &= -((-\Delta_{\mathcal{N}})^{-1}D_2(\rho^{n+1}-\rho^n),\rho^{n+1}-\rho^n)_{\mathcal{N}} \le 0. \end{aligned} \tag{23}$$

Adding (22) and (23) leads to the expected result. □

4.2. Convergence in the optimal rate

Define $H^m_{\mathrm{per}}(\Omega)=\{v\in H^m(\Omega)\,|\,v \text{ is } \Omega\text{-periodic}\}$. Denote by u_e and ρ_e the exact solutions to the binary fluid-surfactant system (2). Given $T>0$ and initial data regular sufficiently, we can assume

$$\begin{cases} u_e\in H^1(0,T;H^{10}_{\mathrm{per}}(\Omega))\cap L^\infty(0,T;H^{m+6}_{\mathrm{per}}(\Omega)),\\ \rho_e\in H^1(0,T;H^{9}_{\mathrm{per}}(\Omega))\cap L^\infty(0,T;H^{m+4}_{\mathrm{per}}(\Omega)). \end{cases} \tag{24}$$

First, we estimate the error between the exact solution $u_e(t)$ or $\rho_e(t)$ and the solution $\widetilde{u}(t)$ or $\widetilde{\rho}(t)$ of the space-discrete problem (13), i.e.,

$$\frac{\mathrm{d}\widetilde{u}}{\mathrm{d}t} = -M_u(\Delta_{\mathcal{N}}^2 - \alpha\Delta_{\mathcal{N}}^3)\widetilde{u} - M_u\Delta_{\mathcal{N}}\Big(-\frac{1}{\epsilon^2}f(\widetilde{u}) - 2\theta\nabla_{\mathcal{N}}\cdot(\widetilde{\rho}\nabla_{\mathcal{N}}\widetilde{u})\Big), \tag{25a}$$

$$\frac{\mathrm{d}\widetilde{\rho}}{\mathrm{d}t} = -M_\rho\beta\Delta_{\mathcal{N}}^2\widetilde{\rho} - M_\rho\Delta_{\mathcal{N}}\Big(-\frac{1}{\eta^2}g(\widetilde{\rho}) + \theta|\nabla_{\mathcal{N}}\widetilde{u}|^2\Big). \tag{25b}$$

Noting that the problem (25) takes the same form as the continuous problem (12) except for the discretized differential operators, it is reasonable to assume the uniform boundedness of $\|\nabla_{\mathcal{N}}\widetilde{u}(t)\|_\infty$ and $\|\widetilde{\rho}(t)\|_\infty$. Denote $f_1 = \max\limits_{u\in\mathbb{R}}|f'(u)| \le 3\gamma_1^2 - 1$ and $g_1 = \max\limits_{u\in\mathbb{R}}|g'(u)| \le 3\gamma_2^2 + 3\gamma_2 + \frac{1}{2}$.

Lemma 4.3. *Assume that $u_e \in L^\infty(0,T;H_{\mathrm{per}}^{m+6}(\Omega))$ and $\rho_e \in L^\infty(0,T;H_{\mathrm{per}}^{m+4}(\Omega))$. For any fixed $t\in(0,T]$, we have*

$$\|u_e(t) - \widetilde{u}(t)\|_{\mathcal{N}} + \|\rho_e(t) - \widetilde{\rho}(t)\|_{\mathcal{N}} \le C^* h^m,$$

where $h = \max\{h_x, h_y\}$ and $C^* > 0$ is a constant independent of h.

Proof. A careful consistency analysis indicates that the exact solution satisfies

$$\frac{\mathrm{d}u_e}{\mathrm{d}t} = -M_u(\Delta_{\mathcal{N}}^2 - \alpha\Delta_{\mathcal{N}}^3)u_e - M_u\Delta_{\mathcal{N}}\Big(-\frac{1}{\epsilon^2}f(u_e) - 2\theta\nabla_{\mathcal{N}}\cdot(\rho_e\nabla_{\mathcal{N}}u_e)\Big) + \tau_u(t), \tag{26a}$$

$$\frac{\mathrm{d}\rho_e}{\mathrm{d}t} = -M_\rho\beta\Delta_{\mathcal{N}}^2\rho_e - M_\rho\Delta_{\mathcal{N}}\Big(-\frac{1}{\eta^2}g(\rho_e) + \theta|\nabla_{\mathcal{N}}u_e|^2\Big) + \tau_\rho(t), \tag{26b}$$

where the truncation errors $\tau_u(t)$ and $\tau_\rho(t)$ satisfy

$$\sup_{t\in(0,T]}\|\tau_u(t)\|_{\mathcal{N}} \le C_* h^m, \quad \sup_{t\in(0,T]}\|\tau_\rho(t)\|_{\mathcal{N}} \le C_* h^m,$$

where $C_* > 0$ is a constant independent on h. Let $\overline{e}_u(t) = u_e(t) - \widetilde{u}(t)$ and $\overline{e}_\rho(t) = \rho_e(t) - \widetilde{\rho}(t)$, $t\in(0,T]$, then the difference between (26) and (25) gives us

$$\frac{\mathrm{d}\overline{e}_u}{\mathrm{d}t} = M_u(\alpha\Delta_{\mathcal{N}}^3 - \Delta_{\mathcal{N}}^2)\overline{e}_u + \frac{M_u}{\epsilon^2}\Delta_{\mathcal{N}}(f(u_e) - f(\widetilde{u})) + 2M_u\theta\Delta_{\mathcal{N}}\nabla_{\mathcal{N}}\cdot(\rho_e\nabla_{\mathcal{N}}u_e - \widetilde{\rho}\nabla_{\mathcal{N}}\widetilde{u}) + \tau_u(t), \tag{27a}$$

$$\frac{\mathrm{d}\overline{e}_\rho}{\mathrm{d}t} = -M_\rho\beta\Delta_{\mathcal{N}}^2\overline{e}_\rho + \frac{M_\rho}{\eta^2}\Delta_{\mathcal{N}}(g(\rho_e) - g(\widetilde{\rho})) + M_\rho\theta\Delta_{\mathcal{N}}(|\nabla_{\mathcal{N}}\widetilde{u}|^2 - |\nabla_{\mathcal{N}}u_e|^2) + \tau_\rho(t). \tag{27b}$$

Taking the discrete L^2 inner product of (27a) with $2\overline{e}_u$, we have

$$\frac{\mathrm{d}}{\mathrm{d}t}\|\overline{e}_u\|_{\mathcal{N}}^2 = -2M_u\|\Delta_{\mathcal{N}}\overline{e}_u\|_{\mathcal{N}}^2 - 2\alpha M_u\|\Delta_{\mathcal{N}}\nabla_{\mathcal{N}}\overline{e}_u\|_{\mathcal{N}}^2 + \mathbf{I}_u + \mathbf{II}_u + \mathbf{III}_u,$$

where

$$\mathbf{III}_u = 2(\tau_u, \overline{e}_u)_{\mathcal{N}} \le \|\tau_u\|_{\mathcal{N}}^2 + \|\overline{e}_u\|_{\mathcal{N}}^2,$$

and

$$\mathbf{I}_u = \frac{2M_u}{\epsilon^2}(f(u_e) - f(\widetilde{u}), \Delta_{\mathcal{N}}\overline{e}_u)_{\mathcal{N}} \le \frac{2M_u}{\epsilon^2}f_1\|\overline{e}_u\|_{\mathcal{N}}\|\Delta_{\mathcal{N}}\overline{e}_u\|_{\mathcal{N}} \le \frac{M_u f_1^2}{\epsilon^4}\|\overline{e}_u\|_{\mathcal{N}}^2 + M_u\|\Delta_{\mathcal{N}}\overline{e}_u\|_{\mathcal{N}}^2.$$

In addition, we derive

$$\begin{aligned}
\mathbf{II}_u &= 4M_u\theta(\rho_e\nabla_{\mathcal{N}}u_e - \widetilde{\rho}\nabla_{\mathcal{N}}\widetilde{u}, \Delta_{\mathcal{N}}\nabla_{\mathcal{N}}\overline{e}_u)_{\mathcal{N}} \\
&= 4M_u\theta(\overline{e}_\rho\nabla_{\mathcal{N}}u_e, \Delta_{\mathcal{N}}\nabla_{\mathcal{N}}\overline{e}_u)_{\mathcal{N}} + 4M_u\theta(\widetilde{\rho}\nabla_{\mathcal{N}}\overline{e}_u, \Delta_{\mathcal{N}}\nabla_{\mathcal{N}}\overline{e}_u)_{\mathcal{N}} \\
&\le \frac{4M_u\theta^2\|\nabla_{\mathcal{N}}u_e\|_\infty^2}{\alpha}\|\overline{e}_\rho\|_{\mathcal{N}}^2 + \alpha M_u\|\Delta_{\mathcal{N}}\nabla_{\mathcal{N}}\overline{e}_u\|_{\mathcal{N}}^2 + \frac{4M_u\theta^2\|\widetilde{\rho}\|_\infty^2}{\alpha}\|\nabla_{\mathcal{N}}\overline{e}_u\|_{\mathcal{N}}^2 + \alpha M_u\|\Delta_{\mathcal{N}}\nabla_{\mathcal{N}}\overline{e}_u\|_{\mathcal{N}}^2
\end{aligned}$$

$$= \frac{4M_u\theta^2\|\nabla_{\mathcal{N}}u_e\|_\infty^2}{\alpha}\|\overline{e}_\rho\|_{\mathcal{N}}^2 + 2\alpha M_u\|\Delta_{\mathcal{N}}\nabla_{\mathcal{N}}\overline{e}_u\|_{\mathcal{N}}^2 - \frac{4M_u\theta^2\|\widetilde{\rho}\|_\infty^2}{\alpha}(\overline{e}_u, \Delta_{\mathcal{N}}\overline{e}_u)$$
$$\leq \frac{4M_u\theta^2\|\nabla_{\mathcal{N}}u_e\|_\infty^2}{\alpha}\|\overline{e}_\rho\|_{\mathcal{N}}^2 + 2\alpha M_u\|\Delta_{\mathcal{N}}\nabla_{\mathcal{N}}\overline{e}_u\|_{\mathcal{N}}^2 + \frac{8M_u\theta^4\|\widetilde{\rho}\|_\infty^4}{\alpha^2}\|\overline{e}_u\|_{\mathcal{N}}^2 + \frac{M_u}{2}\|\Delta_{\mathcal{N}}\overline{e}_u\|_{\mathcal{N}}^2.$$

Thus, we obtain

$$\frac{\mathrm{d}}{\mathrm{d}t}\|\overline{e}_u\|_{\mathcal{N}}^2 + \frac{M_u}{2}\|\Delta_{\mathcal{N}}\overline{e}_u\|_{\mathcal{N}}^2 \leq \Big(\frac{M_u f_1^2}{\epsilon^4} + \frac{8M_u\theta^4\|\widetilde{\rho}\|_\infty^4}{\alpha^2} + 1\Big)\|\overline{e}_u\|_{\mathcal{N}}^2 + \frac{4M_u\theta^2\|\nabla_{\mathcal{N}}u_e\|_\infty^2}{\alpha}\|\overline{e}_\rho\|_{\mathcal{N}}^2 + \|\tau_u\|_{\mathcal{N}}^2. \quad (28)$$

Taking the discrete L^2 inner product of (27b) with $2\overline{e}_\rho$, we have

$$\frac{\mathrm{d}}{\mathrm{d}t}\|\overline{e}_\rho\|_{\mathcal{N}}^2 = -2\beta M_\rho\|\Delta_{\mathcal{N}}\overline{e}_\rho\|_{\mathcal{N}}^2 + \mathbf{I}_\rho + \mathbf{II}_\rho + \mathbf{III}_\rho,$$

where

$$\mathbf{III}_\rho = 2(\tau_\rho, \overline{e}_\rho) \leq \|\tau_\rho\|_{\mathcal{N}}^2 + \|\overline{e}_\rho\|_{\mathcal{N}}^2,$$

and

$$\mathbf{I}_\rho = \frac{2M_\rho}{\eta^2}(g(\rho_e) - g(\widetilde{\rho}), \Delta_{\mathcal{N}}\overline{e}_\rho)_{\mathcal{N}} \leq \frac{2M_\rho}{\eta^2}g_1\|\overline{e}_\rho\|_{\mathcal{N}}\|\Delta_{\mathcal{N}}\overline{e}_\rho\|_{\mathcal{N}} \leq \frac{M_\rho g_1^2}{\beta\eta^4}\|\overline{e}_\rho\|_{\mathcal{N}}^2 + \beta M_\rho\|\Delta_{\mathcal{N}}\overline{e}_\rho\|_{\mathcal{N}}^2.$$

In addition, we have

$$\begin{aligned}
\mathbf{II}_\rho &= 2M_\rho\theta(|\nabla_{\mathcal{N}}\widetilde{u}|^2 - |\nabla_{\mathcal{N}}u_e|^2, \Delta_{\mathcal{N}}\overline{e}_\rho)_{\mathcal{N}} \\
&= -2M_\rho\theta(\nabla_{\mathcal{N}}\overline{e}_u(\nabla_{\mathcal{N}}\widetilde{u} + \nabla_{\mathcal{N}}u_e), \Delta_{\mathcal{N}}\overline{e}_\rho)_{\mathcal{N}} \\
&\leq \frac{M_\rho\theta^2\|\nabla_{\mathcal{N}}\widetilde{u} + \nabla_{\mathcal{N}}u_e\|_\infty^2}{\beta}\|\nabla_{\mathcal{N}}\overline{e}_u\|_{\mathcal{N}}^2 + \beta M_\rho\|\Delta_{\mathcal{N}}\overline{e}_\rho\|_{\mathcal{N}}^2 \\
&\leq \frac{M_\rho^2\theta^4\|\nabla_{\mathcal{N}}\widetilde{u} + \nabla_{\mathcal{N}}u_e\|_\infty^4}{2\beta^2 M_u}\|\overline{e}_u\|_{\mathcal{N}}^2 + \frac{M_u}{2}\|\Delta_{\mathcal{N}}\overline{e}_u\|_{\mathcal{N}}^2 + \beta M_\rho\|\Delta_{\mathcal{N}}\overline{e}_\rho\|_{\mathcal{N}}^2.
\end{aligned}$$

Then, we obtain

$$\frac{\mathrm{d}}{\mathrm{d}t}\|\overline{e}_\rho\|_{\mathcal{N}}^2 - \frac{M_u}{2}\|\Delta_{\mathcal{N}}\overline{e}_u\|_{\mathcal{N}}^2 = \frac{2M_\rho^2\theta^4\|\nabla_{\mathcal{N}}\widetilde{u} + \nabla_{\mathcal{N}}u_e\|_\infty^4}{2\beta^2 M_u}\|\overline{e}_u\|_{\mathcal{N}}^2 + \Big(\frac{M_\rho g_1^2}{\beta\eta^4} + 1\Big)\|\overline{e}_\rho\|_{\mathcal{N}}^2 + \|\tau_\rho\|_{\mathcal{N}}^2. \quad (29)$$

Adding (28) and (29), we obtain

$$\begin{aligned}
\frac{\mathrm{d}}{\mathrm{d}t}\big(\|\overline{e}_u\|_{\mathcal{N}}^2 + \|\overline{e}_\rho\|_{\mathcal{N}}^2\big) \leq{}& \Big(\frac{M_u f_1^2}{\epsilon^4} + \frac{8M_u\theta^4\|\widetilde{\rho}\|_\infty^4}{\alpha^2} + \frac{2M_\rho^2\theta^4\|\nabla_{\mathcal{N}}\widetilde{u} + \nabla_{\mathcal{N}}u_e\|_\infty^4}{2\beta^2 M_u} + 1\Big)\|\overline{e}_u\|_{\mathcal{N}}^2 \\
&+ \Big(\frac{M_\rho g_1^2}{\beta\eta^4} + \frac{4M_u\theta^2\|\nabla_{\mathcal{N}}u_e\|_\infty^2}{\alpha} + 1\Big)\|\overline{e}_\rho\|_{\mathcal{N}}^2 + \|\tau_u\|_{\mathcal{N}}^2 + \|\tau_\rho\|_{\mathcal{N}}^2.
\end{aligned}$$

According to the regularity of u_e and the assumptions of boundedness of $\widetilde{u}$ and $\widetilde{\rho}$, the quantities in the parenthesis are constants independent of t. Then, an application of the Gronwall inequality leads to

$$\|\overline{e}_u(t)\|_{\mathcal{N}} + \|\overline{e}_\rho(t)\|_{\mathcal{N}} \leq C^* h^m, \quad t \in (0, T],$$

where $C^* > 0$ is a constant independent on h. □

Next, we estimate the error between the space-discrete solutions $\widetilde{u}(t)$ and $\widetilde{\rho}(t)$ given by (25) and the approximate solutions u^n and ρ^n computed by the ETD1 scheme (17).

For a linear symmetric positive definite operator $\mathcal{A} : \mathcal{M}_{\mathcal{N}} \to \mathcal{M}_{\mathcal{N}}$, we denote by $|||\mathcal{A}|||$ the spectrum norm of $\mathcal{A}$. It is obvious that $\|\mathcal{A}v\|_{\mathcal{N}} \leq |||\mathcal{A}|||\,\|v\|_{\mathcal{N}}$ for any $v \in \mathcal{M}_{\mathcal{N}}$. We define

$$q_1(a) = (1 + a)\phi_0(-a), \quad q_2(a) = (1 + a)\phi_1(-a),$$

and it is easy to verify that $0 < q_1(a) < 1 < q_2(a) < 2$ for any $a > 0$.

Lemma 4.4. *Suppose the solution to the space-discrete problem* (25) *is regular enough such that* $\Delta_{\mathcal{N}}^5\widetilde{u} \in H^1(0,T;\mathcal{M}_{\mathcal{N}})$ *and* $\nabla_{\mathcal{N}}\Delta_{\mathcal{N}}^4\widetilde{\rho} \in H^1(0,T;\mathcal{M}_{\mathcal{N}})$. *For any positive integer* n *such that* $t_n \le T$, *when* Δt *is small sufficiently, we have*

$$\|\widetilde{u}(t_n) - u^n\|_{\mathcal{N}} + \|\widetilde{\rho}(t_n) - \rho^n\|_{\mathcal{N}} \le C_*\Delta t,$$

where $C_* > 0$ *is a constant independent of* Δt *and* h.

Proof. The solutions $\widetilde{u}(t_n)$ and $\widetilde{\rho}(t_n)$ to the space-discrete problem (25) satisfy

$$\widetilde{u}(t_{n+1}) = \phi_0(-L_{\mathcal{N}}\Delta t)\widetilde{u}(t_n) - \Delta t\phi_1(-L_{\mathcal{N}}\Delta t)f_{\mathcal{N}}(\widetilde{u}(t_n),\widetilde{\rho}(t_{n+1})) + \tau_u^n, \tag{30a}$$
$$\widetilde{\rho}(t_{n+1}) = \phi_0(-K_{\mathcal{N}}\Delta t)\widetilde{\rho}(t_n) - \Delta t\phi_1(-K_{\mathcal{N}}\Delta t)g_{\mathcal{N}}(\widetilde{u}(t_n),\widetilde{\rho}(t_n)) + \tau_\rho^n, \tag{30b}$$

where τ_u^n and τ_ρ^n are the truncation errors given by

$$\tau_u^n = \int_0^{\Delta t} \mathrm{e}^{-L_{\mathcal{N}}(\Delta t - s)}\big(f_{\mathcal{N}}(\widetilde{u}(t_n),\widetilde{\rho}(t_{n+1})) - f_{\mathcal{N}}(\widetilde{u}(t_n+s),\widetilde{\rho}(t_n+s))\big)\,\mathrm{d}s,$$
$$\tau_\rho^n = \int_0^{\Delta t} \mathrm{e}^{-K_{\mathcal{N}}(\Delta t - s)}\big(g_{\mathcal{N}}(\widetilde{u}(t_n),\widetilde{\rho}(t_n)) - g_{\mathcal{N}}(\widetilde{u}(t_n+s),\widetilde{\rho}(t_n+s))\big)\,\mathrm{d}s.$$

By similar analysis as conducted in [15, Lemma 4.2], we can obtain the following estimates:

$$\|(I + L_{\mathcal{N}}\Delta t)\tau_u^n\|_{\mathcal{N}} \le C_0(\Delta t)^2, \qquad \|(I + K_{\mathcal{N}}\Delta t)\tau_\rho^n\|_{\mathcal{N}} \le C_0(\Delta t)^2, \tag{31}$$

where C_0 is a constant depending on the exact solution. Let $\widetilde{e}_u^n = \widetilde{u}(t_n) - u^n$ and $\widetilde{e}_\rho^n = \widetilde{\rho}(t_n) - \rho^n$. Subtracting the ETD1 scheme (17) from the consistency estimate (30) yields

$$\widetilde{e}_u^{n+1} = \phi_0(-L_{\mathcal{N}}\Delta t)\widetilde{e}_u^n - \Delta t\phi_1(-L_{\mathcal{N}}\Delta t)\big(f_{\mathcal{N}}(\widetilde{u}(t_n),\widetilde{\rho}(t_{n+1})) - f_{\mathcal{N}}(u^n,\rho^{n+1})\big) + \tau_u^n, \tag{32a}$$
$$\widetilde{e}_\rho^{n+1} = \phi_0(-K_{\mathcal{N}}\Delta t)\widetilde{e}_\rho^n - \Delta t\phi_1(-K_{\mathcal{N}}\Delta t)\big(g_{\mathcal{N}}(\widetilde{u}(t_n),\widetilde{\rho}(t_n)) - g_{\mathcal{N}}(u^n,\rho^n)\big) + \tau_\rho^n. \tag{32b}$$

Recall that we have assumed the uniform boundedness of $\|\nabla_{\mathcal{N}}\widetilde{u}(t)\|_\infty$ and $\|\widetilde{\rho}(t)\|_\infty$. More precisely, suppose $\|\nabla_{\mathcal{N}}\widetilde{u}(t)\|_\infty + \|\widetilde{\rho}(t)\|_\infty \le C_1$ uniformly in t. In addition, we assume that $\|\nabla_{\mathcal{N}}u^n\|_\infty \le C_2$.

Acting $(I + L_{\mathcal{N}}\Delta t)$ on both sides of (32a) and taking the discrete L^2 inner product of the resulting equality with $\widetilde{e}_u^{n+1}$ yield

$$\begin{aligned}
&\|\widetilde{e}_u^{n+1}\|_{\mathcal{N}}^2 + M_u\kappa_1\Delta t\|\nabla_{\mathcal{N}}\widetilde{e}_u^{n+1}\|_{\mathcal{N}}^2 + M_u\Delta t\|\Delta_{\mathcal{N}}\widetilde{e}_u^{n+1}\|_{\mathcal{N}}^2 + M_u\alpha\Delta t\|\nabla_{\mathcal{N}}\Delta_{\mathcal{N}}\widetilde{e}_u^{n+1}\|_{\mathcal{N}}^2\\
&\quad = \big(q_1(L_{\mathcal{N}}\Delta t)\widetilde{e}_u^n, \widetilde{e}_u^{n+1}\big)_{\mathcal{N}} + \big((I + L_{\mathcal{N}}\Delta t)\tau_u^n, \widetilde{e}_u^{n+1}\big)_{\mathcal{N}}\\
&\qquad - \Delta t\big(q_2(L_{\mathcal{N}}\Delta t)\big(f_{\mathcal{N}}(\widetilde{u}(t_n),\widetilde{\rho}(t_{n+1})) - f_{\mathcal{N}}(u^n,\rho^{n+1})\big), \widetilde{e}_u^{n+1}\big)_{\mathcal{N}}.
\end{aligned} \tag{33}$$

By using the property of the function q_1, the first and second terms on the right-hand side of (33) can be estimated as

$$\big(q_1(L_{\mathcal{N}}\Delta t)\widetilde{e}_u^n, \widetilde{e}_u^{n+1}\big)_{\mathcal{N}} \le \|q_1(L_{\mathcal{N}}\Delta t)\widetilde{e}_u^n\|_{\mathcal{N}}\|\widetilde{e}_u^{n+1}\|_{\mathcal{N}} \le \frac{1}{2}\|\widetilde{e}_u^n\|_{\mathcal{N}}^2 + \frac{1}{2}\|\widetilde{e}_u^{n+1}\|_{\mathcal{N}}^2,$$
$$\big((I + L_{\mathcal{N}}\Delta t)\tau_u^n, \widetilde{e}_u^{n+1}\big)_{\mathcal{N}} \le \|(I + L_{\mathcal{N}}\Delta t)\tau_u^n\|_{\mathcal{N}}\|\widetilde{e}_u^{n+1}\|_{\mathcal{N}} \le \frac{1}{2\Delta t}\|(I + L_{\mathcal{N}}\Delta t)\tau_u^n\|_{\mathcal{N}}^2 + \frac{\Delta t}{2}\|\widetilde{e}_u^{n+1}\|_{\mathcal{N}}^2.$$

We split the third term in (33) into three parts as follows:

$$\begin{aligned}
&-\Delta t\big(q_2(L_{\mathcal{N}}\Delta t)\big(f_{\mathcal{N}}(\widetilde{u}(t_n),\widetilde{\rho}(t_{n+1})) - f_{\mathcal{N}}(u^n,\rho^{n+1})\big), \widetilde{e}_u^{n+1}\big)_{\mathcal{N}}\\
&\quad = \frac{M_u}{\epsilon^2}\Delta t\big(q_2(L_{\mathcal{N}}\Delta t)(f(\widetilde{u}(t_n)) - f(u^n)), \Delta_{\mathcal{N}}\widetilde{e}_u^{n+1}\big)_{\mathcal{N}} - M_u\kappa_1\Delta t\big(q_2(L_{\mathcal{N}}\Delta t)\widetilde{e}_u^n, \Delta_{\mathcal{N}}\widetilde{e}_u^{n+1}\big)_{\mathcal{N}}\\
&\qquad + 2M_u\theta\Delta t\big(q_2(L_{\mathcal{N}}\Delta t)\big(\rho^{n+1}\nabla_{\mathcal{N}}u^n - \widetilde{\rho}(t_{n+1})\nabla_{\mathcal{N}}\widetilde{u}(t_n)\big), \nabla_{\mathcal{N}}\Delta_{\mathcal{N}}\widetilde{e}_u^{n+1}\big)_{\mathcal{N}}\\
&\quad =: \mathbf{I}_u' + \mathbf{II}_u' + \mathbf{III}_u'.
\end{aligned}$$

By the property of the function q_2, we can estimate the terms $\mathbf{I}'_u$ and $\mathbf{II}'_u$ as

$$\begin{aligned}\mathbf{I}'_u &\le \frac{2M_u}{\epsilon^2}\Delta t\|f(\widetilde{u}(t_n)) - f(u^n)\|_{\mathcal{N}}\|\Delta_{\mathcal{N}}\widetilde{e}_u^{n+1}\|_{\mathcal{N}}\\ &\le \frac{2M_u f_1}{\epsilon^2}\Delta t\|\widetilde{e}_u^n\|_{\mathcal{N}}\|\Delta_{\mathcal{N}}\widetilde{e}_u^{n+1}\|_{\mathcal{N}} \le \frac{4M_u f_1^2}{\epsilon^4}\Delta t\|\widetilde{e}_u^n\|_{\mathcal{N}}^2 + \frac{M_u}{4}\Delta t\|\Delta_{\mathcal{N}}\widetilde{e}_u^{n+1}\|_{\mathcal{N}}^2\end{aligned}$$

and

$$\mathbf{II}'_u \le 2M_u\kappa_1\Delta t\|\widetilde{e}_u^n\|_{\mathcal{N}}\|\Delta_{\mathcal{N}}\widetilde{e}_u^{n+1}\|_{\mathcal{N}} \le 4M_u\kappa_1^2\Delta t\|\widetilde{e}_u^n\|_{\mathcal{N}}^2 + \frac{M_u}{4}\Delta t\|\Delta_{\mathcal{N}}\widetilde{e}_u^{n+1}\|_{\mathcal{N}}^2.$$

Some careful calculations give us

$$\begin{aligned}\mathbf{III}'_u &= -2M_u\theta\Delta t\big(q_2(L_{\mathcal{N}}\Delta t)\big(\widetilde{e}_\rho^{n+1}\nabla_{\mathcal{N}}u^n\big), \nabla_{\mathcal{N}}\Delta_{\mathcal{N}}\widetilde{e}_u^{n+1}\big)_{\mathcal{N}}\\ &\quad - 2M_u\theta\Delta t\big(q_2(L_{\mathcal{N}}\Delta t)\big(\widetilde{\rho}(t_{n+1})\nabla_{\mathcal{N}}\widetilde{e}_u^n\big), \nabla_{\mathcal{N}}\Delta_{\mathcal{N}}\widetilde{e}_u^{n+1}\big)_{\mathcal{N}}\\ &\le 4M_u\theta\Delta t\|\nabla_{\mathcal{N}}u^n\|_\infty\|\widetilde{e}_\rho^{n+1}\|_{\mathcal{N}}\|\nabla_{\mathcal{N}}\Delta_{\mathcal{N}}\widetilde{e}_u^{n+1}\|_{\mathcal{N}}\\ &\quad + 4M_u\theta\Delta t\|\widetilde{\rho}(t_{n+1})\|_\infty\|\nabla_{\mathcal{N}}\widetilde{e}_u^n\|_{\mathcal{N}}\|\nabla_{\mathcal{N}}\Delta_{\mathcal{N}}\widetilde{e}_u^{n+1}\|_{\mathcal{N}}\\ &\le \frac{8M_u\theta^2C_2^2}{\alpha}\Delta t\|\widetilde{e}_\rho^{n+1}\|_{\mathcal{N}}^2 + \frac{M_u\alpha}{2}\Delta t\|\nabla_{\mathcal{N}}\Delta_{\mathcal{N}}\widetilde{e}_u^{n+1}\|_{\mathcal{N}}^2\\ &\quad + \frac{8M_u\theta^2C_1^2}{\alpha}\Delta t\|\nabla_{\mathcal{N}}\widetilde{e}_u^n\|_{\mathcal{N}}^2 + \frac{M_u\alpha}{2}\Delta t\|\nabla_{\mathcal{N}}\Delta_{\mathcal{N}}\widetilde{e}_u^{n+1}\|_{\mathcal{N}}^2\\ &\le \frac{8M_u\theta^2C_2^2}{\alpha}\Delta t\|\widetilde{e}_\rho^{n+1}\|_{\mathcal{N}}^2 + M_u\alpha\Delta t\|\nabla_{\mathcal{N}}\Delta_{\mathcal{N}}\widetilde{e}_u^{n+1}\|_{\mathcal{N}}^2 + \frac{8M_u\theta^2C_1^2}{\alpha}\Delta t\|\widetilde{e}_u^n\|_{\mathcal{N}}\|\Delta_{\mathcal{N}}\widetilde{e}_u^n\|_{\mathcal{N}}\\ &\le \frac{8M_u\theta^2C_2^2}{\alpha}\Delta t\|\widetilde{e}_\rho^{n+1}\|_{\mathcal{N}}^2 + M_u\alpha\Delta t\|\nabla_{\mathcal{N}}\Delta_{\mathcal{N}}\widetilde{e}_u^{n+1}\|_{\mathcal{N}}^2 + \frac{64M_u\theta^4C_1^4}{\alpha^2}\Delta t\|\widetilde{e}_u^n\|_{\mathcal{N}}^2 + \frac{M_u}{4}\Delta t\|\Delta_{\mathcal{N}}\widetilde{e}_u^n\|_{\mathcal{N}}^2.\end{aligned}$$

Combining (33) with the above estimates, we obtain

$$\begin{aligned}&\frac{1}{2}\big(\|\widetilde{e}_u^{n+1}\|_{\mathcal{N}}^2 - \|\widetilde{e}_u^n\|_{\mathcal{N}}^2\big) + M_u\kappa_1\Delta t\|\nabla_{\mathcal{N}}\widetilde{e}_u^{n+1}\|_{\mathcal{N}}^2 + \frac{M_u}{2}\Delta t\|\Delta_{\mathcal{N}}\widetilde{e}_u^{n+1}\|_{\mathcal{N}}^2\\ &\quad\le \Big(\frac{4M_u f_1^2}{\epsilon^4} + 4M_u\kappa_1^2 + \frac{64M_u\theta^4C_1^4}{\alpha^2}\Big)\Delta t\|\widetilde{e}_u^n\|_{\mathcal{N}}^2 + \frac{M_u}{4}\Delta t\|\Delta_{\mathcal{N}}\widetilde{e}_u^n\|_{\mathcal{N}}^2\\ &\qquad + \frac{\Delta t}{2}\|\widetilde{e}_u^{n+1}\|_{\mathcal{N}}^2 + \frac{8M_u\theta^2C_2^2}{\alpha}\Delta t\|\widetilde{e}_\rho^{n+1}\|_{\mathcal{N}}^2 + \frac{1}{2\Delta t}\|(I + L_{\mathcal{N}}\Delta t)\tau_u^n\|_{\mathcal{N}}^2.\end{aligned}\tag{34}$$

Acting $(I + K_{\mathcal{N}}\Delta t)$ on both sides of (32b) and taking the discrete L^2 inner product with $\widetilde{e}_\rho^{n+1}$ give us

$$\begin{aligned}&\|\widetilde{e}_\rho^{n+1}\|_{\mathcal{N}}^2 + M_\rho\kappa_2\Delta t\|\nabla_{\mathcal{N}}\widetilde{e}_\rho^{n+1}\|_{\mathcal{N}}^2 + M_\rho\beta\Delta t\|\Delta_{\mathcal{N}}\widetilde{e}_\rho^{n+1}\|_{\mathcal{N}}^2\\ &\quad= \big(q_1(K_{\mathcal{N}}\Delta t)\widetilde{e}_\rho^n, \widetilde{e}_\rho^{n+1}\big)_{\mathcal{N}} + \big((I + K_{\mathcal{N}}\Delta t)\tau_\rho^n, \widetilde{e}_\rho^{n+1}\big)_{\mathcal{N}}\\ &\qquad - \Delta t\big(q_2(K_{\mathcal{N}}\Delta t)\big(g_{\mathcal{N}}(\widetilde{u}(t_n), \widetilde{\rho}(t_n)) - g_{\mathcal{N}}(u^n, \rho^n)\big), \widetilde{e}_\rho^{n+1}\big)_{\mathcal{N}},\end{aligned}\tag{35}$$

where the first two terms on the right-hand side can be estimated as

$$\begin{aligned}\big(q_1(K_{\mathcal{N}}\Delta t)\widetilde{e}_\rho^n, \widetilde{e}_\rho^{n+1}\big)_{\mathcal{N}} &\le \|q_1(K_{\mathcal{N}}\Delta t)\widetilde{e}_\rho^n\|_{\mathcal{N}}\|\widetilde{e}_\rho^{n+1}\|_{\mathcal{N}} \le \frac{1}{2}\|\widetilde{e}_\rho^n\|_{\mathcal{N}}^2 + \frac{1}{2}\|\widetilde{e}_\rho^{n+1}\|_{\mathcal{N}}^2,\\ \big((I + K_{\mathcal{N}}\Delta t)\tau_\rho^n, \widetilde{e}_\rho^{n+1}\big)_{\mathcal{N}} &\le \|(I + K_{\mathcal{N}}\Delta t)\tau_\rho^n\|_{\mathcal{N}}\|\widetilde{e}_\rho^{n+1}\|_{\mathcal{N}} \le \frac{1}{2\Delta t}\|(I + K_{\mathcal{N}}\Delta t)\tau_\rho^n\|_{\mathcal{N}}^2 + \frac{\Delta t}{2}\|\widetilde{e}_\rho^{n+1}\|_{\mathcal{N}}^2,\end{aligned}$$

and the third term is decomposed into three parts as follows:

$$\begin{aligned}&-\Delta t\big(q_2(K_{\mathcal{N}}\Delta t)\big(g_{\mathcal{N}}(\widetilde{u}(t_n), \widetilde{\rho}(t_n)) - g_{\mathcal{N}}(u^n, \rho^n)\big), \widetilde{e}_\rho^{n+1}\big)_{\mathcal{N}}\\ &\quad= \frac{M_\rho}{\eta^2}\Delta t\big(q_2(K_{\mathcal{N}}\Delta t)(g(\widetilde{\rho}(t_n)) - g(\rho^n)), \Delta_{\mathcal{N}}\widetilde{e}_\rho^{n+1}\big)_{\mathcal{N}} - M_\rho\kappa_2\Delta t\big(q_2(K_{\mathcal{N}}\Delta t)\widetilde{e}_\rho^n, \Delta_{\mathcal{N}}\widetilde{e}_\rho^{n+1}\big)_{\mathcal{N}}\end{aligned}$$

$$
\begin{aligned}
&+ M_\rho\theta\Delta t\big(q_2(K_{\mathcal{N}}\Delta t)\big(|\nabla_{\mathcal{N}}u^n|^2 - |\nabla_{\mathcal{N}}\widetilde{u}(t_n)|^2\big), \Delta_{\mathcal{N}}\widetilde{e}_\rho^{n+1}\big)_{\mathcal{N}}\\
&=: \mathbf{I}'_\rho + \mathbf{II}'_\rho + \mathbf{III}'_\rho.
\end{aligned}
$$

Similar to the estimates of $\mathbf{I}'_u$ and $\mathbf{II}'_u$ as above, we derive

$$
\begin{aligned}
\mathbf{I}'_\rho &\le \frac{4M_\rho g_1^2}{\beta\eta^4}\Delta t\|\widetilde{e}_\rho^n\|_{\mathcal{N}}^2 + \frac{M_\rho\beta}{4}\Delta t\|\Delta_{\mathcal{N}}\widetilde{e}_\rho^{n+1}\|_{\mathcal{N}}^2,\\
\mathbf{II}'_\rho &\le \frac{4M_\rho\kappa_2^2}{\beta}\Delta t\|\widetilde{e}_\rho^n\|_{\mathcal{N}}^2 + \frac{M_\rho\beta}{4}\Delta t\|\Delta_{\mathcal{N}}\widetilde{e}_\rho^{n+1}\|_{\mathcal{N}}^2.
\end{aligned}
$$

In addition, the term $\mathbf{III}'_\rho$ can be estimated as follows:

$$
\begin{aligned}
\mathbf{III}'_\rho &= -M_\rho\theta\Delta t\big(q_2(K_{\mathcal{N}}\Delta t)\big((\nabla_{\mathcal{N}}u^n + \nabla_{\mathcal{N}}\widetilde{u}(t_n))\cdot\nabla_{\mathcal{N}}\widetilde{e}_u^n\big), \Delta_{\mathcal{N}}\widetilde{e}_\rho^{n+1}\big)_{\mathcal{N}}\\
&\le 2M_\rho\theta\Delta t\|\nabla_{\mathcal{N}}u^n + \nabla_{\mathcal{N}}\widetilde{u}(t_n)\|_\infty\|\nabla_{\mathcal{N}}\widetilde{e}_u^n\|_{\mathcal{N}}\|\Delta_{\mathcal{N}}\widetilde{e}_\rho^{n+1}\|_{\mathcal{N}}\\
&\le \frac{4M_\rho\theta^2(C_1+C_2)^2}{\beta}\Delta t\|\nabla_{\mathcal{N}}\widetilde{e}_u^n\|_{\mathcal{N}}^2 + \frac{M_\rho\beta}{4}\Delta t\|\Delta_{\mathcal{N}}\widetilde{e}_\rho^{n+1}\|_{\mathcal{N}}^2\\
&\le \frac{4M_\rho\theta^2(C_1+C_2)^2}{\beta}\Delta t\|\widetilde{e}_u^n\|_{\mathcal{N}}\|\Delta_{\mathcal{N}}\widetilde{e}_u^n\|_{\mathcal{N}} + \frac{M_\rho\beta}{4}\Delta t\|\Delta_{\mathcal{N}}\widetilde{e}_\rho^{n+1}\|_{\mathcal{N}}^2\\
&\le \frac{16M_\rho^2\theta^4(C_1+C_2)^4}{\beta^2M_u}\Delta t\|\widetilde{e}_u^n\|_{\mathcal{N}}^2 + \frac{M_u}{4}\Delta t\|\Delta_{\mathcal{N}}\widetilde{e}_u^n\|_{\mathcal{N}}^2 + \frac{M_\rho\beta}{4}\Delta t\|\Delta_{\mathcal{N}}\widetilde{e}_\rho^{n+1}\|_{\mathcal{N}}^2.
\end{aligned}
$$

Combining (35) with the above estimates, we obtain

$$
\begin{aligned}
&\frac{1}{2}\big(\|\widetilde{e}_\rho^{n+1}\|_{\mathcal{N}}^2 - \|\widetilde{e}_\rho^n\|_{\mathcal{N}}^2\big) + M_\rho\kappa_2\Delta t\|\nabla_{\mathcal{N}}\widetilde{e}_\rho^{n+1}\|_{\mathcal{N}}^2 + \frac{M_\rho\beta}{4}\Delta t\|\Delta_{\mathcal{N}}\widetilde{e}_\rho^{n+1}\|_{\mathcal{N}}^2\\
&\quad\le \frac{16M_\rho^2\theta^4(C_1+C_2)^4}{\beta^2M_u}\Delta t\|\widetilde{e}_u^n\|_{\mathcal{N}}^2 + \Big(\frac{4M_\rho g_1^2}{\beta\eta^4} + \frac{4M_\rho\kappa_2^2}{\beta}\Big)\Delta t\|\widetilde{e}_\rho^n\|_{\mathcal{N}}^2\\
&\qquad + \frac{\Delta t}{2}\|\widetilde{e}_\rho^{n+1}\|_{\mathcal{N}}^2 + \frac{M_u}{4}\Delta t\|\Delta_{\mathcal{N}}\widetilde{e}_u^n\|_{\mathcal{N}}^2 + \frac{1}{2\Delta t}\|(I + K_{\mathcal{N}}\Delta t)\tau_\rho^n\|_{\mathcal{N}}^2. \qquad (36)
\end{aligned}
$$

Adding (34) and (36) leads to

$$
\begin{aligned}
&\frac{1}{2}\big(\|\widetilde{e}_u^{n+1}\|_{\mathcal{N}}^2 - \|\widetilde{e}_u^n\|_{\mathcal{N}}^2\big) + \frac{1}{2}\big(\|\widetilde{e}_\rho^{n+1}\|_{\mathcal{N}}^2 - \|\widetilde{e}_\rho^n\|_{\mathcal{N}}^2\big) + \frac{M_u}{2}\Delta t\big(\|\Delta_{\mathcal{N}}\widetilde{e}_u^{n+1}\|_{\mathcal{N}}^2 - \|\Delta_{\mathcal{N}}\widetilde{e}_u^n\|_{\mathcal{N}}^2\big)\\
&+ M_u\kappa_1\Delta t\|\nabla_{\mathcal{N}}\widetilde{e}_u^{n+1}\|_{\mathcal{N}}^2 + M_\rho\kappa_2\Delta t\|\nabla_{\mathcal{N}}\widetilde{e}_\rho^{n+1}\|_{\mathcal{N}}^2 + \frac{M_\rho\beta}{4}\Delta t\|\Delta_{\mathcal{N}}\widetilde{e}_\rho^{n+1}\|_{\mathcal{N}}^2\\
&\quad\le \Big(\frac{4M_u f_1^2}{\epsilon^4} + 4M_u\kappa_1^2 + \frac{64M_u\theta^4C_1^4}{\alpha^2} + \frac{16M_\rho^2\theta^4(C_1+C_2)^4}{\beta^2M_u}\Big)\Delta t\|\widetilde{e}_u^n\|_{\mathcal{N}}^2\\
&\qquad + \Big(\frac{4M_\rho g_1^2}{\beta\eta^4} + \frac{4M_\rho\kappa_2^2}{\beta}\Big)\Delta t\|\widetilde{e}_\rho^n\|_{\mathcal{N}}^2 + \frac{\Delta t}{2}\|\widetilde{e}_u^{n+1}\|_{\mathcal{N}}^2 + \Big(\frac{8M_u\theta^2C_2^2}{\alpha} + \frac{1}{2}\Big)\Delta t\|\widetilde{e}_\rho^{n+1}\|_{\mathcal{N}}^2\\
&\qquad + \frac{1}{2\Delta t}\|(I + L_{\mathcal{N}}\Delta t)\tau_u^n\|_{\mathcal{N}}^2 + \frac{1}{2\Delta t}\|(I + K_{\mathcal{N}}\Delta t)\tau_\rho^n\|_{\mathcal{N}}^2.
\end{aligned}
$$

Summing the above inequality from 0 to n and using the estimates (31), we obtain

$$
\begin{aligned}
&\frac{1}{2}\big(\|\widetilde{e}_u^{n+1}\|_{\mathcal{N}}^2 + \|\widetilde{e}_\rho^{n+1}\|_{\mathcal{N}}^2 + M_u\Delta t\|\Delta_{\mathcal{N}}\widetilde{e}_u^{n+1}\|_{\mathcal{N}}^2\big)\\
&+ M_u\kappa_1\Delta t\sum_{k=1}^{n+1}\|\nabla_{\mathcal{N}}\widetilde{e}_u^k\|_{\mathcal{N}}^2 + M_\rho\kappa_2\Delta t\sum_{k=1}^{n+1}\|\nabla_{\mathcal{N}}\widetilde{e}_\rho^k\|_{\mathcal{N}}^2 + \frac{M_\rho\beta}{4}\Delta t\sum_{k=1}^{n+1}\|\Delta_{\mathcal{N}}\widetilde{e}_\rho^k\|_{\mathcal{N}}^2\\
&\quad\le \Big(\frac{4M_u f_1^2}{\epsilon^4} + 4M_u\kappa_1^2 + \frac{64M_u\theta^4C_1^4}{\alpha^2} + \frac{16M_\rho^2\theta^4(C_1+C_2)^4}{\beta^2M_u} + \frac{1}{2}\Big)\Delta t\sum_{k=1}^{n}\|\widetilde{e}_u^k\|_{\mathcal{N}}^2
\end{aligned}
$$

$$+\Big(\frac{4M_\rho g_1^2}{\beta\eta^4}+\frac{4M_\rho\kappa_2^2}{\beta}+\frac{8M_u\theta^2C_2^2}{\alpha}+\frac{1}{2}\Big)\Delta t\sum_{k=1}^{n}\|\widetilde{e}_\rho^k\|_{\mathcal{N}}^2$$
$$+\frac{\Delta t}{2}\|\widetilde{e}_u^{n+1}\|_{\mathcal{N}}^2+\Big(\frac{8M_u\theta^2C_2^2}{\alpha}+\frac{1}{2}\Big)\Delta t\|\widetilde{e}_\rho^{n+1}\|_{\mathcal{N}}^2+C_0^2T(\Delta t)^2.$$

Dropping off the nonnegative terms on the left-hand side, the above inequality can be simplified as

$$\begin{aligned}(1-\Delta t)\|\widetilde{e}_u^{n+1}\|_{\mathcal{N}}^2+\Big[1-\Big(\frac{16M_u\theta^2C_2^2}{\alpha}+1\Big)\Delta t\Big]\|\widetilde{e}_\rho^{n+1}\|_{\mathcal{N}}^2\\ \le\Big(\frac{8M_uf_1^2}{\epsilon^4}+8M_u\kappa_1^2+\frac{128M_u\theta^4C_1^4}{\alpha^2}+\frac{32M_\rho^2\theta^4(C_1+C_2)^4}{\beta^2M_u}+1\Big)\Delta t\sum_{k=1}^{n}\|\widetilde{e}_u^k\|_{\mathcal{N}}^2\\ +\Big(\frac{8M_\rho g_1^2}{\beta\eta^4}+\frac{8M_\rho\kappa_2^2}{\beta}+\frac{16M_u\theta^2C_2^2}{\alpha}+\Big)\Delta t\sum_{k=1}^{n}\|\widetilde{e}_\rho^k\|_{\mathcal{N}}^2+2C_0^2T(\Delta t)^2.\end{aligned}$$

When Δt is small sufficiently, an application of the discrete Gronwall inequality results in

$$\|\widetilde{e}_u^{n+1}\|_{\mathcal{N}}^2+\|\widetilde{e}_\rho^{n+1}\|_{\mathcal{N}}^2\le C(\Delta t)^2,$$

where $C>0$ is a constant independent on Δt. □

Finally, combining Lemmas 4.3 and 4.4 leads to the following fully discrete error estimate.

Theorem 4.5. *Suppose the exact solution to binary fluid-surfactant system* (2) *satisfies the regularity* (24). *For any positive integer n such that $t_n\le T$, when Δt is small sufficiently, we have*

$$\|u_e(t_n)-u^n\|_{\mathcal{N}}+\|\rho_e(t_n)-\rho^n\|_{\mathcal{N}}\le C(\Delta t+h^m),$$

where $C>0$ is independent of Δt, h and n.

Remark 4.1. We made an assumption $\|\nabla_{\mathcal{N}}u^n\|_{\mathcal{N}}\le C_2$ in the proof of Lemma 4.4. In fact, such an assumption can be removed if we conduct more technical analysis. Note that this assumption is enforced to the numerical solution at the previous time step t_n, and the result of the proof of Lemma 4.4 is the error estimate of the solution at the next step t_{n+1}, which means that the numerical solution u^{n+1} is close to the exact solution in some sense. With the help of the inverse estimate and the embedding theorem, we may derive the boundedness of $\|\nabla_{\mathcal{N}}u^{n+1}\|_{\mathcal{N}}$. Therefore, the convergence analysis can be carried out in the induction way with the uniform boundedness of $\|\nabla_{\mathcal{N}}u^n\|_{\mathcal{N}}$ as a byproduct. Such analysis is beyond the scope of this paper, and we refer interested readers to the literature (e.g., [11, 12, 23, 24]) for the similar technical details.

5. Numerical experiments

In this section, we perform numerical experiments for the ETD1 scheme (17) to verify the previous theoretical results, including the energy stability and the accuracy in time. Though we do not prove the uniform boundedness of the numerical solutions u^n and ρ^n, a large amount of numerical experiments indicate that the numerical solutions are always bounded in practice. According to Remark 3.1, it suffices to set $\gamma_1=2$ and $\gamma_2=1$ so that the numerical solutions are always located in the ranges where the nonlinear terms $f(u)$ and $g(\rho)$ take the original forms without modifications. And thus, by (3), we set $\kappa_1=11/\epsilon^2$ and $\kappa_2=6.5/\eta^2$ unless there are specific statements. The computed domain is $\Omega=[0,2\pi]^2$ and the periodic boundary condition is imposed. The values of the parameters are given as follows:

$$M_u=2.5\times10^{-4},\ M_\rho=2.5\times10^{-4},\ \alpha=2.5\times10^{-4},\ \beta=1,\ \epsilon=0.05,\ \eta=0.08,\ \theta=0.3.$$

We use 128×128 Fourier modes. The time step size $\Delta t=0.001$ is always adopted in all the numerical results below except the accuracy test. For the comparisons, we will also conduct the same experiments by applying

the first-order invariant energy quadratization (IEQ1) scheme developed in [34], where the linear system is solved by the conjugate gradient method with the tolerance 10^{-5}. We will find that the ETD1 scheme with $\Delta t = 0.001$ has the same magnitude of the error as the IEQ1 scheme with $\Delta t = 0.01$. Nevertheless, the ETD1 scheme still performs higher effectiveness than the IEQ1 scheme.

Example 5.1 (Accuracy test). *The initial profiles for u and ρ are chosen as:*

$$u_0(x, y) = 0.3 + 0.01\cos(6x)\cos(6y),$$
$$\rho_0(x, y) = 0.1 + 0.01\cos(6x)\cos(6y).$$

We perform the refinement test of the time step size, and choose the approximate solution obtained by the time step size $\Delta t = 10^{-7}$ as the benchmark solution for computing errors. In Table 1, we display the L^2 errors computed by using the ETD1 scheme. It is observed that the numerical accuracy is about first order in time, which is consistent with the theoretical result. In addition, the numerical error of the ETD1 scheme with $\Delta t = 0.001$ has the same magnitude as that of the IEQ1 scheme with $\Delta t = 0.01$ reported in [34]. This is reasonable because the artificial stabilization terms may introduce the extra truncation errors.

Table 1: Example 5.1: The L^2 errors for u and ρ at $t = 0.1$ computed by ETD1 scheme.

Δt	Error(u)	Rate(u)	Error(ρ)	Rate(ρ)
1e-3	7.6963e-4	–	4.4139e-5	–
5e-4	3.9210e-4	0.9730	2.2116e-5	0.9970
2.5e-4	1.9789e-4	0.9865	1.1068e-5	0.9987
1.25e-4	9.9379e-5	0.9937	5.5349e-6	0.9998
6.25e-5	4.9769e-5	0.9977	2.7660e-6	1.0008
3.125e-5	2.4875e-5	1.0006	1.3810e-6	1.0021
1.5625e-5	1.2405e-5	1.0038	6.8832e-7	1.0045

Figure 1 displays the evolutions of u and ρ fields with the surfactant uniformly distributed over a two-dimensional domain initially. It is observed that a lot of separate ordered patterns formed quickly in the early stage. Then, driven by the energy, some smaller patterns shrink to disappear and some larger patterns are developed due to the conservation of mass until the system reaches the steady state. The surfactant attached to the vanishing patterns will be absorbed into other interfaces nearby. These numerical results are reasonable and consistent with those reported in the literature [10].

Example 5.2 (Stability test). *We set the initial conditions for u and ρ as*

$$u_0(x, y) = 0.3\cos(3x) + 0.5\cos(y),$$
$$\rho_0(x, y) = 0.2\sin(2x) + 0.25\sin(y).$$

In Figure 2, we present the energy development from $t = 0$ to $t = 5$ obtained using various time step sizes. It is found that as the time step size becomes smaller, the curves perform a better-behaved tendency of convergence, which indicates the ETD1 scheme is reasonable. In addition, the curve corresponding to $\Delta t = 0.001$ is close to that for the IEQ1 scheme with $\Delta t = 0.01$, and this is consistent with what we have found in the accuracy test.

We also test the effects of the stabilizing parameters κ_1 and κ_2. As we can see in Figure 3, within some appropriate range, the ETD1 scheme is not sensitive to anyone of κ_1 and κ_2 if we keep the other fixed, which means both parameters are adjustable in a rather large range.

In Figure 4, we present the error evolutions of the total mass of u and ρ, respectively. Obviously, the numerical errors reach the scale 10^{-13}, which shows that the ETD1 scheme is mass-conserved.

Example 5.3 (Coarsening dynamics). *The initial conditions are given by the randomly perturbed concentration fields:*

$$u_0(x, y) = a + 0.001\,\mathrm{rand}(x, y),$$

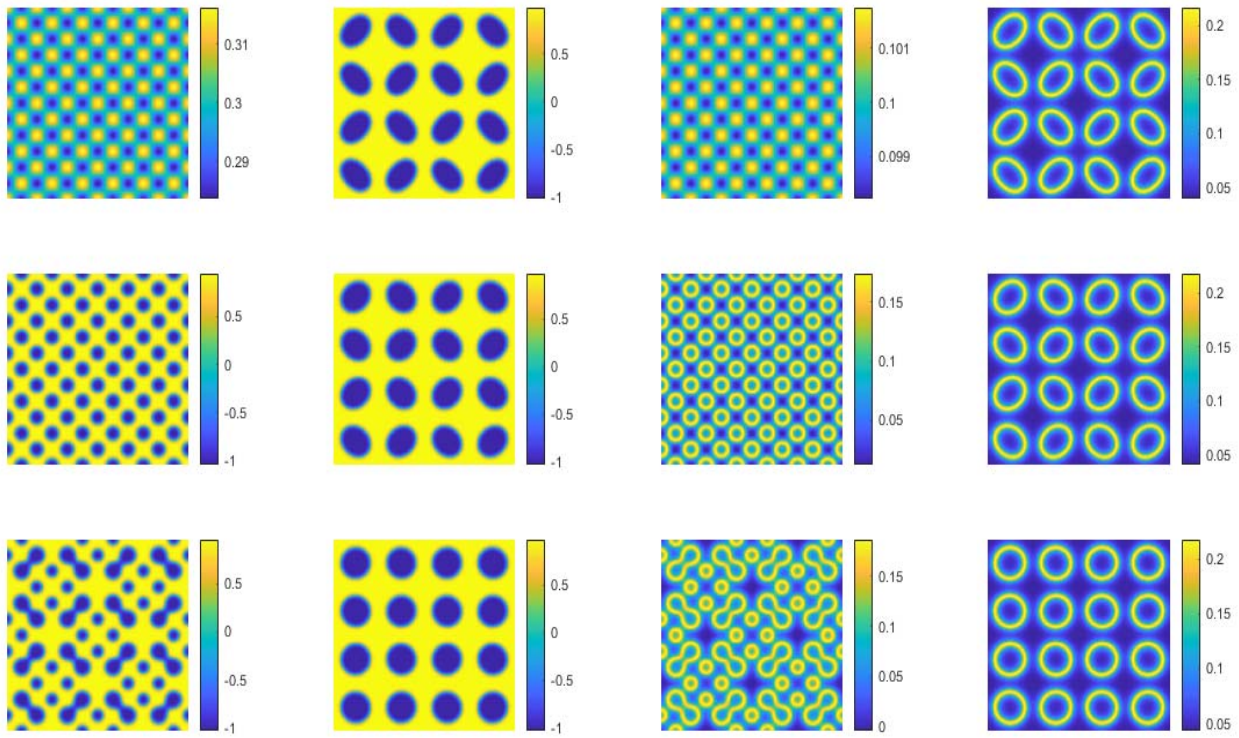

Figure 1: Example 5.1: The first and second columns are the profiles of u at $t = 1$, 50, 200, 220, 250, and 350 (top to bottom and left to right). The third and fourth columns are the profile of ρ at the corresponding moments.

$$\rho_0(x, y) = 0.2 + 0.001\,\mathrm{rand}(x, y),$$

where the function $\mathrm{rand}(x, y)$ *is to produce random numbers in* $[-1, 1]$ *with zero mean.*

We will adopt the ETD1 and IEQ1 schemes to conduct the simulations, where the latter is only used to compare the elapsed CPU time, and all the results shown below are given by the ETD1 scheme. The calculations are conducted in MATLAB on a computer with an Intel 3.60GHz Processor and 32GB Memory.

In Figure 5, we plot the evolutions of energy curves with various choices of the constant a in the initial data. It is seen that the energy has a quick decay in the early stage, and then becomes flat gradually until the steady state is reached.

We show the numerical solutions of u and ρ under the random initial conditions in Figures 6–8. In Figure 6, we show the snapshots of coarsening dynamics with $a = 0$, which means the immiscible fluids (e.g., oil and water) have the same volume. At the beginning, two fluids are well mixed, and then the phase separation occurs and the patterns form quickly. During this early stage, the corresponding energy has a sharp decay, see Figure 5. It is observed that a relatively large value of the variable ρ is located near the interface. The equilibrium state is reached after $t = 1500$, where a banded-shape configuration is formed.

The results for $a = 0.2$ and $a = -0.5$ are given in Figures 7 and 8, respectively. It is observed that the fluid component with less volume accumulates to small droplets. The dynamics are completely different from the previous one. As the time evolves, the small droplets collide, merge and form larger droplets. The final equilibrium state is reached after $t = 1500$, where all droplets accumulate into a big bubble. The results are reasonable and consistent with the reference data reported in [34].

Finally, we report the elapsed CPU times for the ETD1 and IEQ1 simulations up to $t = 2000$. By using the ETD1 scheme with $\Delta t = 0.001$, the average of the elapsed CPU times for the cases $a = 0$, $a = 0.2$ and $a = -0.5$ is about 8.94 hours. Using the IEQ1 scheme with $\Delta t = 0.01$, the average of the elapsed CPU times is about 18.89 hours. We find that, even though a smaller time step is required for the sake of the accuracy,

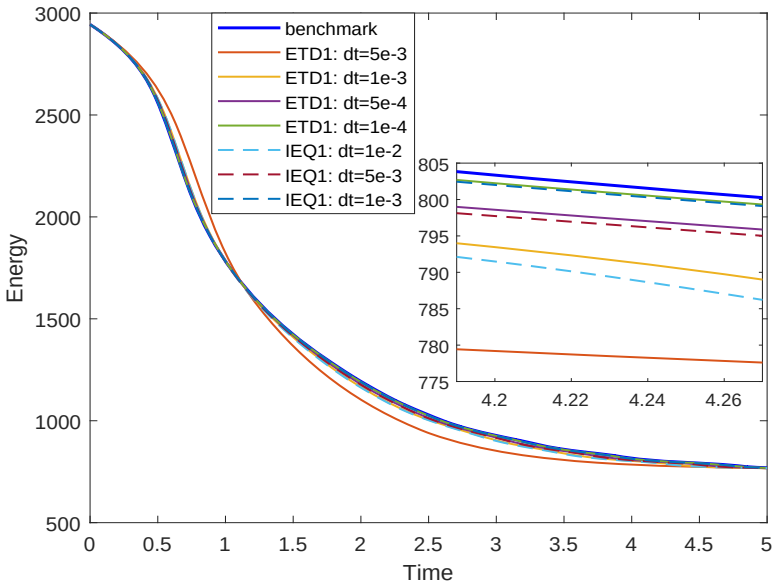

Figure 2: Example 5.2: Evolutions of the free energies.

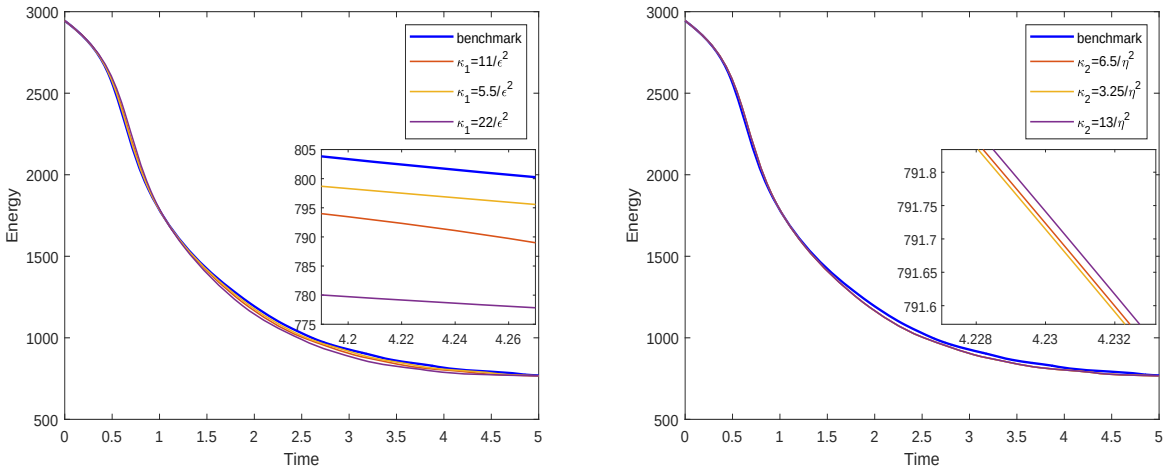

Figure 3: Example 5.2: Evolutions of the free energies for various parameters (left: $\kappa_2 = 6.5/\eta^2$; right: $\kappa_1 = 11/\epsilon^2$).

the ETD1 scheme saves half of the CPU time in comparison with the IEQ1 scheme, which implies the high efficiency of the ETD1 scheme.

6. Concluding remarks

In this paper, we propose the first-order ETD scheme for the Cahn–Hilliard phase field model of binary fluid-surfactant system. The energy functional of two variables and the complexity of nonlinearity make the system very challenging in both theoretical analysis and numerical simulations. In order to overcome this subtle difficulty, we first apply the convex splitting method to the two-dimensional energy functional, and divide each equation in the system into the linear and nonlinear parts. Then, based on the ETD framework,

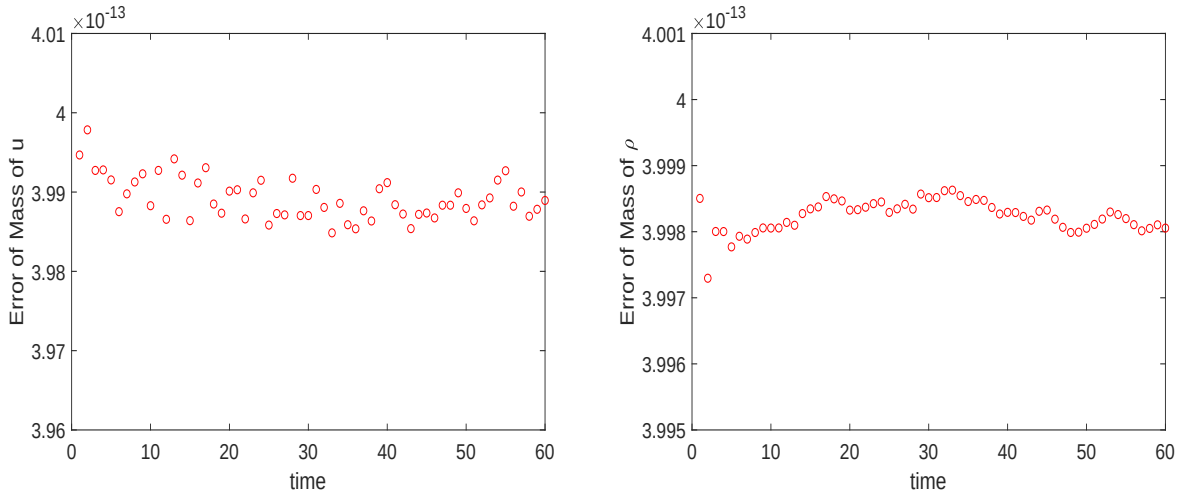

Figure 4: Example 5.2: Evolutions of the errors of the total mass of u and ρ.

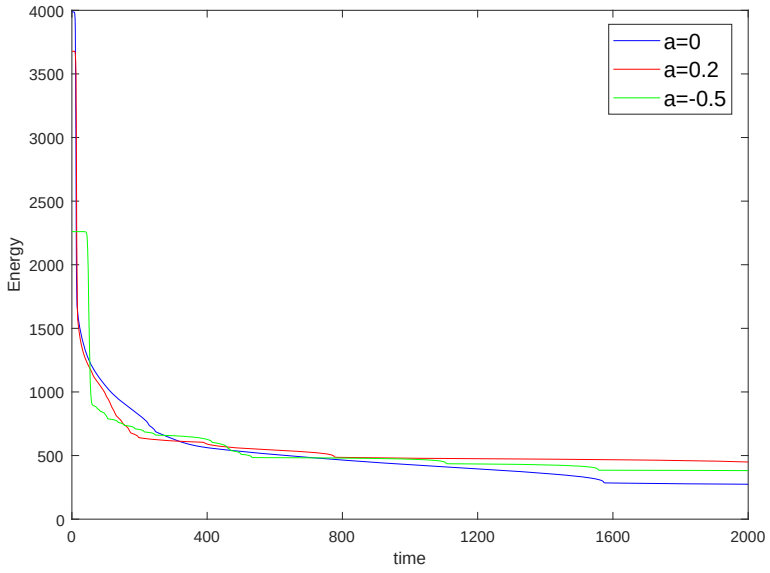

Figure 5: Example 5.3: Evolutions of the free energies.

we propose the first-order ETD scheme. In the numerical analysis part, the unconditional energy stability and the convergence are proved in details. Numerical experiments clearly show the convergence rate of the scheme and the simulated results are in good agreement with those in the literature. To the best of our knowledge, this is the first attempt to apply the ETD method to the Cahn–Hilliard phase field model of binary fluid-surfactant system. It is hopeful to extend the ETD schemes to the case of multivariate energy functionals.

We focus only on the numerical analysis of the first-order ETD scheme in this paper, and we have used relatively small time step sizes in practical computations for the sake of the accuracy. Nevertheless, benefiting from the availability of combining some fast algorithms (such as the FFT we have used), the first-order ETD scheme still performs the satisfactory efficiency in comparison with some other first-order and linear schemes,

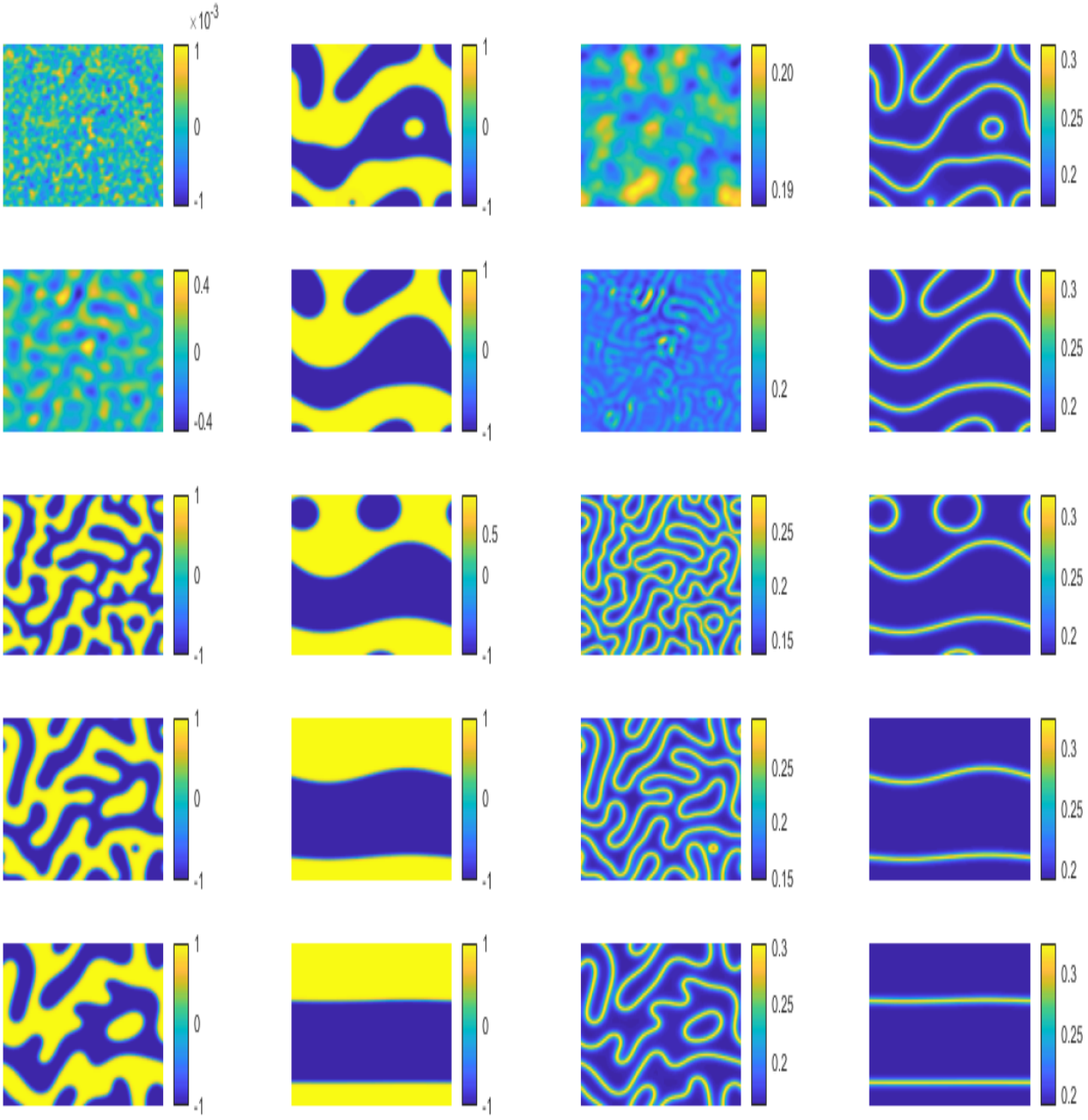

Figure 6: Example 5.3 with $a = 0$: The first and second columns are the profiles of u at $t = 1$, 10, 20, 50, 100, 200, 400, 1000, 1500, and 2000 (top to bottom and left to right). The third and fourth columns are the profile of ρ at the corresponding moments.

as shown by the above numerical experiments. With few difficulties, one can also apply the higher-order methods, such as the second-order ETD multistep method (16), to develop the fully discrete ETD schemes with higher-order temporal accuracy. However, for the second-order and higher-order ETD schemes, there will be some essential difficulties in the analysis on the energy stability and the convergence because of the complicated nonlinear terms, and the corresponding exploration will be left as one of our future works.

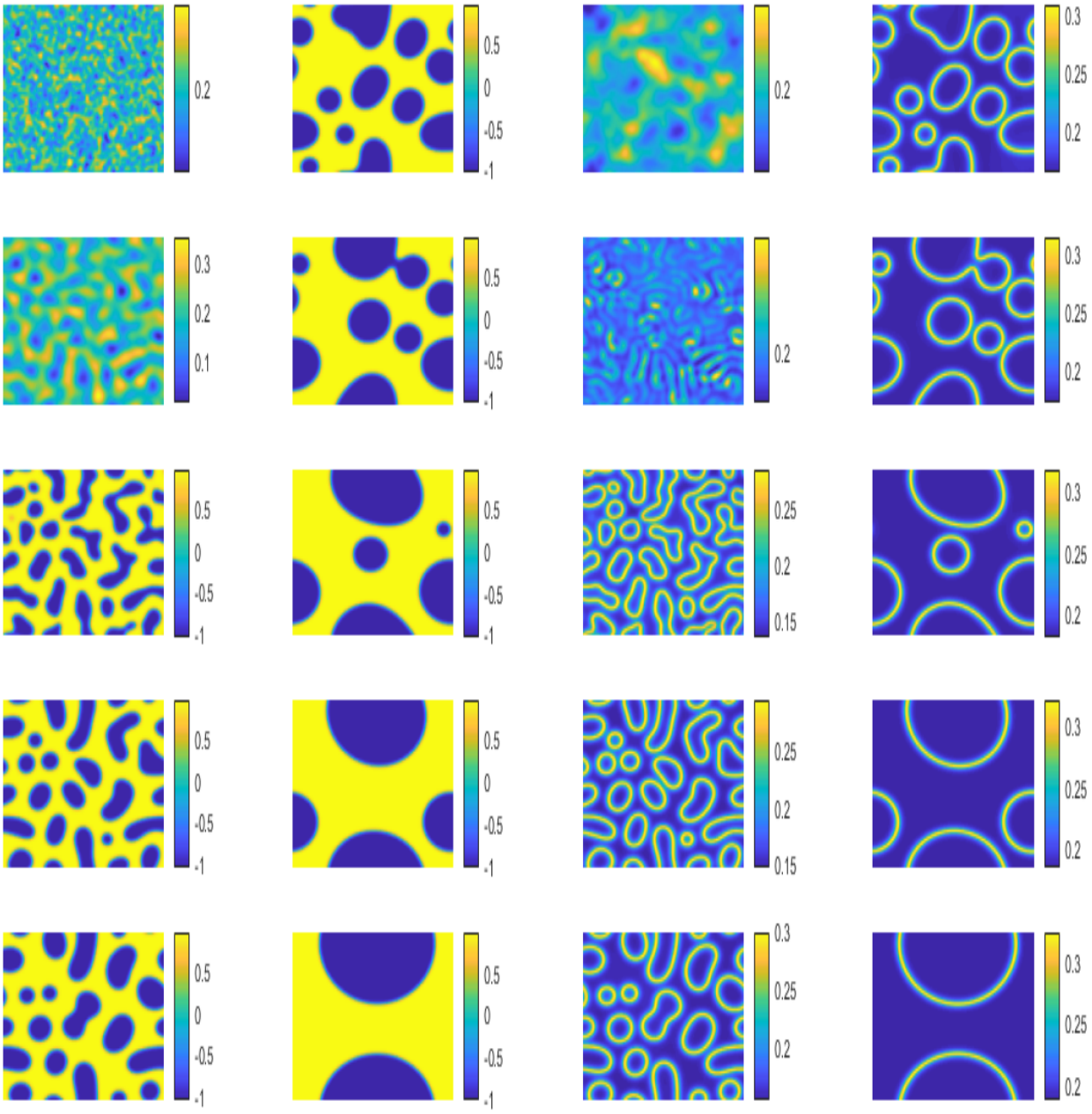

Figure 7: Example 5.3 with $a = 0.2$: The first and second columns are the profiles of u at $t = 1$, 10, 20, 50, 100, 200, 400, 1000, 1500, and 2000 (top to bottom and left to right). The third and fourth columns are the profile of ρ at the corresponding moments.

Acknowledgments

This work is supported in part by the Hong Kong Research Grants Council GRF grant 15300821, and the Hong Kong Polytechnic University grants 1-BD8N, 4-ZZMK, and 1-ZVWW (X. Li), the Hong Kong Research Grant Council RFS grant RFS2021-5S03 and GRF grant 15303121, the Hong Kong Polytechnic University grant 4-ZZLS, and CAS AMSS-PolyU Joint Laboratory of Applied Mathematics (Z.H. Qiao), the NSFC No. 11871105 and 12231003 (Z.R. Zhang).

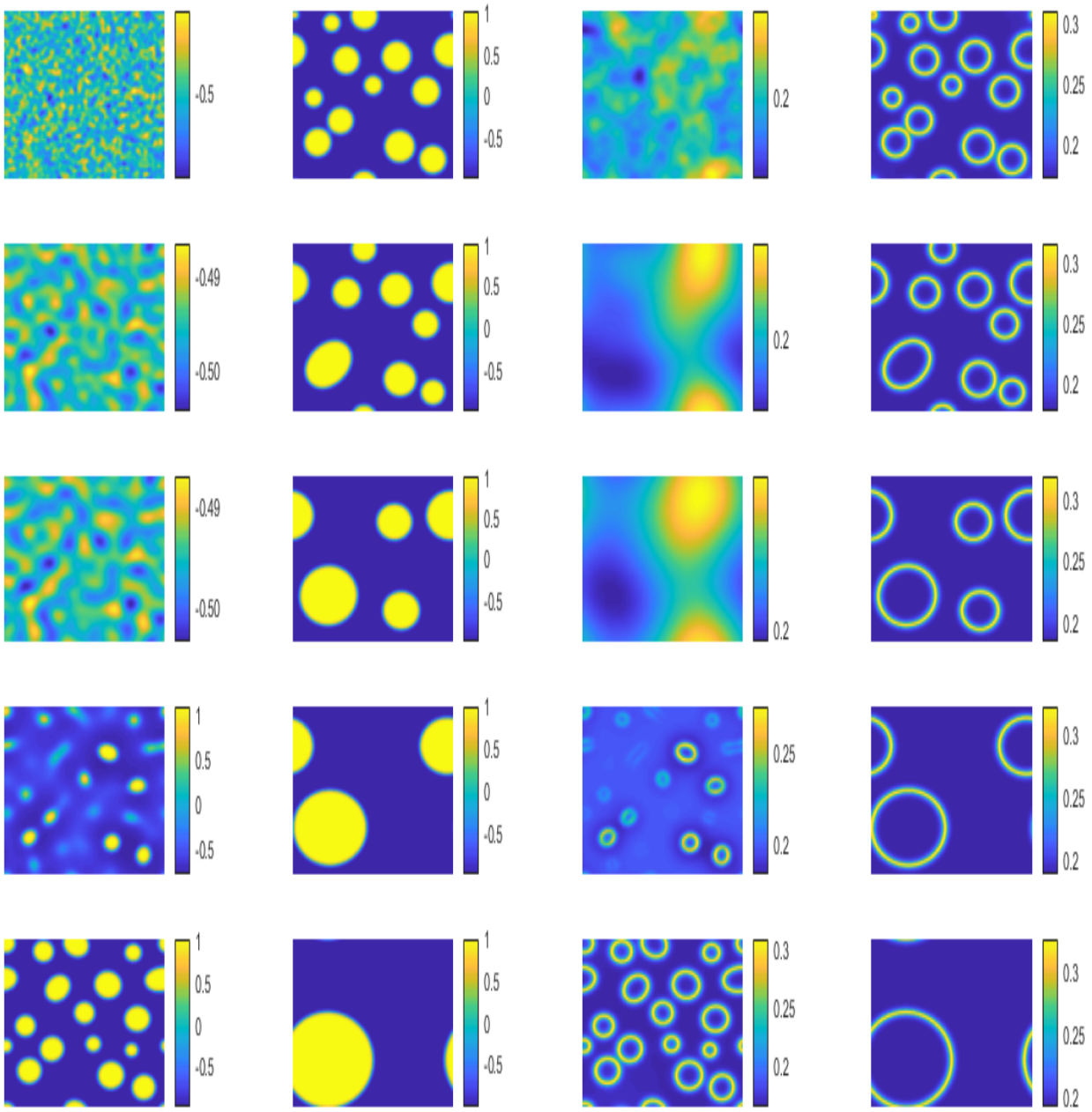

Figure 8: Example 5.3 with $a = -0.5$: The first and second columns are the profiles of u at $t = 1$, 10, 20, 50, 100, 200, 400, 1000, 1500, and 2000 (top to bottom and left to right). The third and fourth columns are the profile of ρ at the corresponding moments.

References

References

[1] K.L. Cheng, Z.H. Qiao, and C. Wang, A third order exponential time differencing numerical scheme for no-slope-selection epitaxial thin film model with energy stability, J. Sci. Comput., 81 (2019), 154–185.

[2] S.M. Cox and P.C. Matthews, Exponential time differencing for stiff systems, J. Comput. Phys., 176 (2002), 430–455.

[3] Q. Du, L. Ju, X. Li, and Z.H. Qiao, Maximum principle preserving exponential time differencing schemes for the nonlocal Allen-Cahn equations, SIAM J. Numer. Anal., 57 (2019), 875–898.

[4] Q. Du and W.X. Zhu, Stability analysis and application of the exponential time differencing schemes, J. Comput. Math., 22 (2004), 200–209.

[5] D. Eyre, Unconditionally gradient stable time marching the Cahn-Hilliard equation, MRS Proceedings, 529 (1998), 39.

[6] X.B. Feng and A. Prol, Numerical analysis of the Allen-Cahn equation and approximation for mean curvature flows, Numer. Math., 94 (2003), 33–65.

[7] I. Fonseca, M. Morini, and V. Slastikov, Surfactants in foam stability: a phase-field approach, Arch. Ration. Mech. Anal., 183 (2007), 411–456.

[8] Z.H. Fu and J. Yang, Energy-decreasing exponential time differencing Runge-Kutta methods for phase-field models, J. Comput. Phys., 454 (2022), 110943.

[9] G. Gompper and M. Schick, Self-assembling amphiphilic systems, In: C. Domb and J. Lebowitz (eds.), Phase transitions and critical phenomena, vol. 16, Academic Press, London, 1994.

[10] S.T. Gu, H. Zhang, and Z.R. Zhang, An energy-stable finite-difference scheme for the binary fluid-surfactant system, J. Comput. Phys., 270 (2014), 416–431.

[11] Z. Guan, J. Lowengrub, and C. Wang, Convergence analysis for second-order accurate schemes for the periodic nonlocal Allen-Cahn and Cahn-Hilliard equations, Math. Methods Appl. Sci., 40 (2017), 6836–6863.

[12] Z. Guan, C. Wang, and S.M. Wise, A convergent convex splitting scheme for the periodic nonlocal Cahn-Hilliard equation, Numer. Math., 128 (2014), 377–406.

[13] N.J. Higham, Functions of Matrices: Theory and Computation, SIAM, Philadelphia, PA, 2008.

[14] M. Hochbruck and A. Ostermann, Exponential integrators, Acta Numer., 19 (2010), 209–286.

[15] L. Ju, X. Li, Z.H. Qiao, and H. Zhang, Energy stability and error estimates of exponential time differencing schemes for the epitaxial growth model without slope selection, Math. Comput., 87 (2018), 1859–1885.

[16] L. Ju, X. Liu, and W. Leng, Compact implicit integration factor methods for a family of semilinear fourth order parabolic equations, Disc. Cont. Dyn. Sys. B, 19 (2014), 1667–1687.

[17] L. Ju, J. Zhang, and Q. Du, Fast and accurate algorithms for simulating coarsening dynamics of Cahn-Hilliard equations, Comput. Mat. Sci., 108 (2015), 272–282.

[18] L. Ju, J. Zhang, L.Y. Zhu, and Q. Du, Fast explicit integration factor methods for semilinear parabolic equations, J. Sci. Comput., 62 (2015), 431–455.

[19] A.-K. Kassam and L.N. Trefethen, Fourth-order time-stepping for stiff PDEs, SIAM J. Sci. Comput., 26 (2005), 1214–1233.

[20] S. Komura and H. Kodama, Two-order-parameter model for an oil-water-surfactant system, Phys. Rev. E, 55 (1997), 1722–1727.

[21] M. Laradji, H. Guo, M. Grant, and M.J. Zuckermann, The effect of surfactants on the dynamics of phase separation, J. Phys. Condens. Matter., 4 (1992), 6715–6728.

[22] M. Laradji, O.G. Mouristen, S. Toxvaerd, and M.J. Zuckermann, Molecular dynamics simulations of phase separation in the presence of surfactants, Phys. Rev. E, 50 (1994), 1722–1727.

[23] X. Li, Z.H. Qiao, and C. Wang, Convergence analysis for a stabilized linear semi-implicit numerical scheme for the nonlocal Cahn-Hilliard equation, Math. Comp., 90 (2021), 327, 171–188.

[24] X. Li, Z.H. Qiao, and C. Wang, Stabilization parameter analysis of a second-order linear numerical scheme for the nonlocal Cahn-Hilliard equation, IMA J. Numer. Anal., 2023, doi: 10.1093/imanum/drab109.

[25] S. Pei, Y. Hou, and B. You, *A linearly second-order energy stable scheme for the phase field crystal model*, Appl. Numer. Math., 140 (2019), 134–164.

[26] Y.Z. Qin, Z. Xu, H. Zhang, and Z.R. Zhang, Fully decoupled, linear and unconditionally energy stable schemes for the binary fluid-surfactant model, Commum. Comput. Phys., 28 (2020), 1389–1414.

[27] Y.Z. Qin, C. Wang, and Z.R. Zhang, A positivity-preserving and convergent numerical scheme for the binary fluid-surfactant system, Int. J. Numer. Anal. Model., 18 (2021), 399–425.

[28] J. Shen, T. Tang, and L.-L. Wang, Spectral Methods: Algorithms, Analysis and Applications, Springer, Heidelberg, 2011.

[29] J. Shen and X.F. Yang, Numerical approximations of Allen-Cahn and Cahn-Hilliard equations, Disc. Cont. Dyn. Sys. A, 28 (2010), 1669-1691.

[30] C.H. Teng, I.L. Chern, and M.C. Lai, Simulating binary fluid-surfactant dynamics by a phase field model, Disc. Cont. Dyn. Sys. B, 17 (2012), 1289–1307.

[31] T. Teramoto and F. Yonezawa, Droplet growth dynamics in a water/oil/surfactant system, J. Colloid Interface Sci., 235 (2001), 329–333.

[32] L.N. Trefethen, Spectral Methods in MATLAB, SIAM, Philadelphia, PA, 2000.

[33] S.M. Wise, C. Wang, and J.S. Lowengrub, An energy-stable and convergent finite-difference scheme for the phase field crystal equation, SIAM J. Numer. Anal., 47 (2009), 2269–2288.

[34] X.F. Yang, Numerical approximations for the Cahn-Hilliard phase field model of the binary fluid-surfactant system, J. Sci. Comput., 74 (2018), 1533–1553.

[35] X.F. Yang and L. Ju, Linear and unconditionally energy stable schemes for the binary fluid-surfactant phase field model, Comput. Methods Appl. Mech. Engrg., 318 (2017), 1005–1029.

[36] G.P. Zhu, J.S. Kou, S.Y. Sun, J. Yao, and A.F. Li, Decoupled, energy stable schemes for a phase-field surfactant model, Comput. Phys. Commun., 233 (2018), 67–77.